HYDROLOGICAL PROCESSES
Hydrol. Process. **12**, 2339–2367 (1998)

An evaluation of snow accumulation and ablation processes for land surface modelling

J. W. Pomeroy[1]*, D. M. Gray[2], K. R. Shook[2], B. Toth[2], R. L. H. Essery[2], A. Pietroniro[1] and N. Hedstrom[1]

[1]*National Hydrology Research Centre, 11 Innovation Blvd, Saskatoon, Saskatchewan S7N 3H5, Canada*
[2]*Division of Hydrology, University of Saskatchewan, Saskatoon,Saskatchewan S7N 0W0, Canada*

Abstract:

This paper discusses the development and testing of snow algorithms with specific reference to their use and application in land surface models. New algorithms, developed by the authors, for estimating snow interception in forest canopies, blowing snow transport and sublimation, snow cover depletion and open environment snowmelt are compared with field measurements. Existing algorithms are discussed and compared with field observations. Recommendations are made with respect to: (a) density of new and aged snow in open and forest environments; (b) interception of snow by evergreen canopies; (c) redistribution and sublimation of snow water equivalent by blowing snow; (d) depletion in snow-covered area during snowmelt; (e) albedo decay during snowmelt; (f) turbulent transfer during snowmelt; and (g) soil heat flux during meltwater infiltration into frozen soils.

Preliminary evidence is presented, suggesting that one relatively advanced land surface model, CLASS, significantly underestimates the timing of snowmelt and snowmelt rates in open environments despite overestimating radiation and turbulent contributions to melt. The cause(s) may be due to overestimation of ground heat loss and other factors. It is recommended that further studies of snow energetics and soil heat transfer in frozen soils be undertaken to provide improvements for land surface models such as CLASS, with particular attention paid to establishing the reliability of the models in invoking closure of the energy equation.

KEY WORDS snow hydrology; general circulation models; CLASS; land surface schemes; energy balance

INTRODUCTION

Algorithms that describe snow processes are important components of land surface schemes for general circulation models (GCMs) because much of the Earth's land surface is covered with snow and ice and strong snow–climate feedbacks have been identified from model output (Cess *et al*., 1991; Thomas and Rowntree, 1992; Randall *et al*., 1994) and measurements (Karl *et al*., 1993). Land surface models have been used as the surface interface for GCMs and are proposed as the modelling interface between the hydrological and atmospheric systems in coupled atmospheric/hydrological models. As the demand for more sophisticated and physically realistic land surface models increases, so does the need to assess current algorithms and recommend the next phase of improvements. The objectives of this paper are: to examine several snow processes that are important in the prairie, boreal forest and arctic environments; to evaluate popular algorithms describing these processes, in particular one relatively advanced model, the Canadian Land Surface Scheme, CLASS (Verseghy, 1991; Verseghy *et al*., 1993); and to recommend new process-based

* Correspondence to: Dr J. W. Pomeroy, National Water Research Institute, National Hydrology Research Centre, Environment Canada, 11 Innovation Blvd, Saskatoon, Saskatchewan S7N 3H5, Canada. Email: john.pomeroy@ec.gc.ca

CCC 0885–6087/98/152339–29$17·50

Received 6 August 1998
Accepted 24 September 1998

algorithms developed from the authors' studies where applicable. Whilst a selection of the many other models are referred to (e.g. Simple Biosphere Model, SiB, Sellers *et al.*, 1996; Max-Planck-Institut, MPI, Loth *et al.*, 1993; European Centre for Medium-Range Weather Forecast, ECMWF, Viterbo and Beljaars, 1995; Interaction between Soil, Biosphere and Atmosphere, ISBA, Douville *et al.*, 1995; United Kingdom Meteorological Office, UKMO, Essery, 1997; National Center for Atmospheric Research, NCAR, Marshall and Oglesby, 1994), CLASS algorithms are selected for attention because they treat snow processes in a comprehensive manner compared with many other land surface schemes, and they should be expected to work well in Canadian environments.

The snow processes considered here include: (a) snow interception by forest canopies, (b) snow redistribution and sublimation by blowing snow, (c) snow densification and depth variability, (d) depletion in snow-covered area during ablation, (e) decay in the albedo of patchy snow covers during melt and (f) melting of complete snow covers. Comparisons are made of process-based algorithms, land surface scheme algorithms and model diagnostic output with field data collected in northern prairie, arctic and southern boreal forest environments over several decades. To illustrate the difficulty in evaluating improvements to complex snow models, the changes to CLASS snow calculations that occur when a new process algorithm is coded into CLASS 2.6 are demonstrated.

EXPERIMENTAL SITES AND DATA COLLECTION

Sites

Sites for data collection were chosen in the prairie (Bad Lake/Saskatoon), boreal forest (Waskesiu) and arctic (Trail Valley) regions of western and northern Canada. All locations experience several continental climates with winter temperatures ranging from just above 0 °C down to approximately −40 °C and relatively low annual snowfall. The mean corrected annual snowfall totals (in terms of water equivalent) at the three sites are of the order of: Bad Lake/Saskatoon, 120 mm; Waskesiu, 150 mm; and Trail Valley, 170 mm.

Waskesiu, Saskatchewan: Beartrap Creek. The Beartrap Creek Basin (53·9°N, 106·1°W, 550 m a.s.l.) is located near Waskesiu within Prince Albert National Park. Sites in this basin were instrumented in 1992 for a series of forest hydrological process experiments for the Canadian GEWEX and Prince Albert Model Forest studies. The region is dominated by mixed-wood southern boreal forest. Its climate is continental boreal with cold winters and snow cover from late October to April (Harding and Pomeroy, 1996; Pomeroy and Dion, 1996; Pomeroy *et al.*, 1997a).

Experiments were conducted from a tower in a mature jack pine (*Pinus banksia*) stand in the Beartrap Creek. The site is level, has a winter leaf + steam area of 2·2 m^2/m^2, a canopy coverage of 82% and an average tree height of 19 ± 3 m. Over the period of study, from November 1994 to April 1995, the low lying carpet of sphagnum moss and kinnikinnick (bearberry) was covered by snow.

Saskatoon, Saskatchewan: Kernen Farm. The Kernen Farm, located just east of the city of Saskatoon (52 °N, 107 °W, 500 m a.s.l.) is an experimental research farm operated by the University of Saskatchewan. It is situated on a flat, open, lacustrine plain, which is cropped to cereal grains and pulse crops under dryland farming. The climate of the area is subhumid and typical of the northern prairie–parkland transition, with cold winters and snow cover from November to March/April. Experiments were conducted in March 1994 and 1996 on fallow and stubble fields on snow accumulation, snow cover depletion, areal albedo and the energetics of snowmelt (Shook, 1995; Shook and Gray, 1997).

Inuvik, Northwest Territories: Trail Valley Creek. The Trail Valley Creek basin (68 °45′N, 133 °30′W, 150 m a.s.l.) located 50 km north of Inuvik, was instrumented for hydrological process and basin modelling experiments in 1991. Currently, these studies form part of the Canadian GEWEX programme. The basin has a low arctic climate with snow cover from September to May. Vegetation is predominately tundra (70%)

interspersed with large areas of shrub tundra (21%) and small pockets of transitional forest tundra (1%) (Marsh and Pomeroy, 1996). The basin has high rolling plateaux, with incised valleys running east–west. Shrubs and forest dominate slopes and valley bottoms, whilst tundra dominates the plateaux. Deep snow drifts, which accumulate in the lee of abrupt changes in topography, cover about 8% of the basin (Pomeroy *et al*., 1997b). Experiments were conducted using observations of micrometeorological variables made from a tower located on a tundra plain with excellent open, uniform fetch characteristics.

Bad Lake, Saskatchewan: Creighton Watershed, Smith Tributary. The Bad Lake Watershed (51 °23′N, 108 °26′W, 650 m a.s.l.) in south-western Saskatchewan was established as a research basin under the International Hydrological Decade Programme and instrumented for hydrological research, beginning in the late 1960s. The basin is largely cultivated (*c*. 70% of the area) in the production of cereal grains, pulses and legumes by dryland farming. Of the remaining area, 20% is rangeland and 10% is native shrub, grass and farmyards. The topography of the basin ranges from poorly drained, level plains to moderately and steeply rolling upland areas, such as the Creighton and Smith tributaries, which contain deeply incised channels. Its climate is semi-arid and typical of northern grasslands, with dry, cold winters and hot summers. Snow covers on the basin exhibit high seasonal and interannual variability. In high snow years, the snow cover normally forms in November and disappears in April, in years with light snows the snow cover forms and ablates several times over the winter, with final ablation in March. During low snow years, the major accumulations are found in waterways and within and surrounding windbreaks owing to redistribution of the snowfall by wind. Experiments to measure snow-covered area, small-scale and large-scale albedo and surface energy balance were conducted during snowmelt periods in 1972 and 1973 (O'Neill, 1972; O'Neill and Gray, 1973). In 1973 and 1974 extensive snow surveys were conducted over various landscape types during midwinter and during the snowmelt period (Steppuhn and Dyck, 1974).

Methodology

Meteorological stations. At Waskesiu, a variety of meteorological instruments were mounted on the 27 m tower in the centre of the pine stand (Pomeroy *et al*., 1997a). Parameters used to run CLASS (radiation, air temperature, humidity, wind speed) were measured above the forest canopy. At the top of the tower, two 'Kipp and Zonen' short-wave radiometers and one 'Middleton' net radiometer measured the incoming and reflected short-wave radiation and net radiation, respectively. The radiometers were cleaned weekly and often more frequently when snowfall occurred. Air temperature/humidity was measured using a 'Vaisala' HMP35CF hygrothermometer and wind speed was measured using a 'Weathertronics' cup anemometer. In addition, the ground heat flux was measured using REBS heat flux plates and snow and soil temperatures were measured using thermocouples. Campbell 21x microloggers were used to control instruments and record data.

At Saskatoon and Trail Valley Creek, 3 m towers were erected in large, uniform, open, snow-covered plains. Similar equipment to that used at Waskesiu was deployed along with an eddy correlation system at Saskatoon. This system comprised a 'Solent' ultrasonic anemometer and a 'Campbell Scientific' Krypton fast hygrometer. Instantaneous measurements of vertical wind speed, air temperature and specific humidity were made at 10 Hz and covariance was calculated over 15 minutes. The eddy correlation system and all other equipment were controlled and logged by Campbell 21x microloggers (Shook and Gray, 1997).

At Bad Lake, similar radiation equipment was employed over grassland along with standard meteorological equipment on a 10 m tower used in a climatological station operated by the Atmospheric Environment Service, Environment Canada (Gray and Granger, 1988). The site is treeless with excellent fetch. Snow depth and soil temperature were also monitored.

Snow fall, accumulation and interception. Snowfall measurements were made with Nipher-shielded AES-style cylinders emptied daily (Bad Lake) or weekly (Waskesiu) or as necessary (Inuvik). The readings were corrected for wind-induced undercatch by procedures described by Goodison *et al*. (1998). At Waskesiu,

half-hourly estimates of snowfall rate were made using a snow particle detector (Brown and Pomeroy, 1989), whose counts were given a mass based on weekly snowfall. Snow accumulation was determined from areal snow surveys following the recommendations listed by Pomeroy and Gray (1995). Ten-point snow surveys under the pine canopy were used in Waskesiu, whilst longer (+100 point) surveys were used in open environments.

Interception was determined from the difference between snowfall and subcanopy snowfall or from the weight of snow on a suspended pine tree, weighed with a load cell at Waskesiu (Hedstrom and Pomeroy, 1998). To provide areal averages of snowfall, subcanopy snowfall was compared to the accumulations determined by snow survey during cold periods and adjusted to provide an areal indicator of subcanopy snowfall. The difference between snowfall and areally averaged subcanopy snowfall was related to the weight of snow on the suspended tree just after new snow events. The ratio of the difference to weight was used to estimate the canopy snow interception load in mm snow water equivalent.

SNOW ACCUMULATION PROCESSES

Snow interception

Interception by forest canopies can store up to 60% of cumulative snowfall by midwinter in cold boreal forests, which results in a 30–40% annual loss of snow cover over the winter in many coniferous forest environments (Pomeroy and Gray, 1995). Following interception, most snow remains in the canopy where it is exposed to a relatively warm and dry atmosphere (Lundberg and Halldin, 1994). As a result, relatively high rates of sublimation occur from intercepted snow, and more snow sublimates than eventually unloads to the surface (Pomeroy and Schmidt, 1993; Pomeroy and Gray, 1995; Harding and Pomeroy, 1996). In order to calculate the amount of sublimation from intercepted snow, it is important to know the amount of snow collected in the canopy so that appropriate exposure times can be determined. For example, given a constant sublimation rate, an underestimation of interception will result in a shorter exposure time for sublimation and a decrease in seasonal sublimation.

Most land surface schemes do not separate canopy snow from surface snow. CLASS and SiB do consider canopy snow load, but consider the snow interception process in a similar manner to rainfall interception. For instance, CLASS calculates snow interception as a linear function of snowfall, with a maximum intercepted snow depth (kg/m^2) equal to 0·2LAI, where LAI is the leaf area index (m^2/m^2).

Field data on snow interception collected for a pine forest in Beartrap Creek, Saskatchewan are shown in Figure 1. Interception measured by Nipher-shielded *snow gauges* is for periods where there were no major releases or unloading of intercepted snow. Interception measured via a *weighed tree* is expressed as an areal average snow water equivalent, SWE. It is seen that as much as 9 mm SWE can be intercepted in this canopy and that interception increases with snowfall up to snowfall amounts of about 16 mm SWE, above which interception does not increase further. CLASS-modelled interception for a such a stand would reach a maximum of 0·44 kg/m^2, more than an order of magnitude less than the measured interception.

The CLASS snow interception routines produce results that are at odds with measured interception for snowfall events larger than about 3 mm snow water equivalent (SWE[1]). As a result, daily snow accumulation fluxes in coniferous forests are misrepresented. To remedy this situation the following snow interception routine, which is a simplification of that developed by Hedstrom and Pomeroy (1998), is recommended. The routine is consistent with field observations that snow interception efficiency decreases with snow canopy load and snowfall amount and increases with canopy density (Pomeroy and Gray, 1995; Hedstrom and Pomeroy, 1998). Modelling this behaviour provides interception, I (kg/m^2), as a function of a dimensionless snow unloading coefficient, c, the difference of the maximum snow load, I^*, and initial snow load, I_0 (kg/m^2),

[1] Snow water equivalent, or SWE, is expressed as mm of equivalent water per unit area or, alternatively, as kg/m^2 of snow.

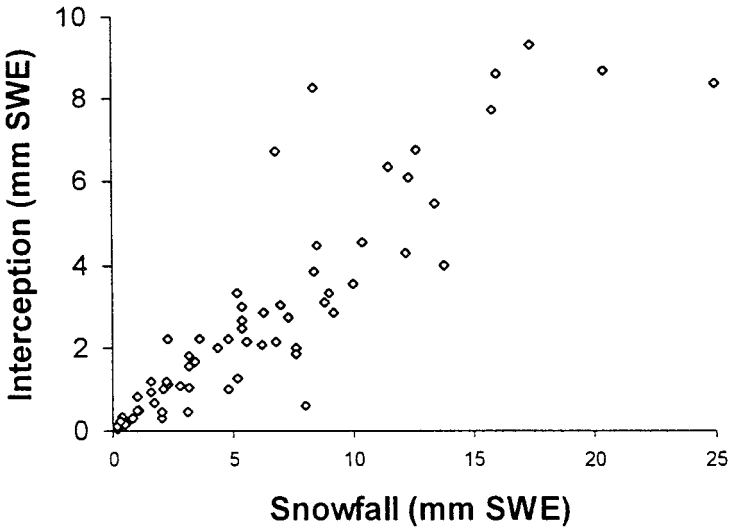

Figure 1. Snow interception of jack pine canopy at Waskesiu, Saskatchewan, measured using the difference in above and below canopy snowfall, converted to areal SWE using snow survey measurements (Hedstrom and Pomeroy, 1998)

an exponential function of snowfall, P (kg/m^2 for a unit time), and the canopy density, C_c (proportional coverage) as (Hedstrom and Pomeroy, 1998):

$$I = c(I^* - I_0)\left(1 - e^{-C_c P/I^*}\right) \tag{1}$$

This expression is independent of time-step except for the unloading coefficient, c. Empirical evidence suggests that a value of $c = 0{\cdot}7$ is appropriate for hourly time-steps. I^* is found as a function of LAI (m^2/m^2), a tree species coefficient, S_p (kg/m^2) and fresh snow density, ρ_s (kg/m^3) following Hedstrom and Pomeroy (1998)

$$I^* = S_p LAI\left(0{\cdot}27 + \frac{46}{\rho_s}\right) \tag{2}$$

Schmidt and Gluns (1991) present field measurements that suggest values for S_p of 6·6 for pine and 5·9 kg/m^2 for spruce. The values for coefficients and constants in Equation (2) are empirically derived and hence based on the units expressed above.

The process-based snow interception routine specifies increasing interception efficiency with LAI and decreasing efficiency with increasing snowfall and initial interception as shown in Figure 2 for a pine canopy. A comparison of modelled and measured snow interception (Figure 3) shows that this is in agreement with the observed behaviour of snow interception in boreal forest environments.

Blowing snow

Redistribution of snow by wind relocates snow covers and produces notable intransit sublimation of blowing snow (Dyunin, 1959; Schmidt, 1972; Pomeroy, 1989). Relocation involves a horizontal mass flux of snow proportional to the fourth power of wind speed, and sublimation of a vertical flux of water vapour proportional to the fifth power of wind speed, depending on fetch. The snow accumulation flux, Q_A, over some fetch distance, F, during blowing snow may be described as

$$Q_A(F) = P - \frac{Q_R(F) - Q_R(0)}{F} - Q_E \tag{3}$$

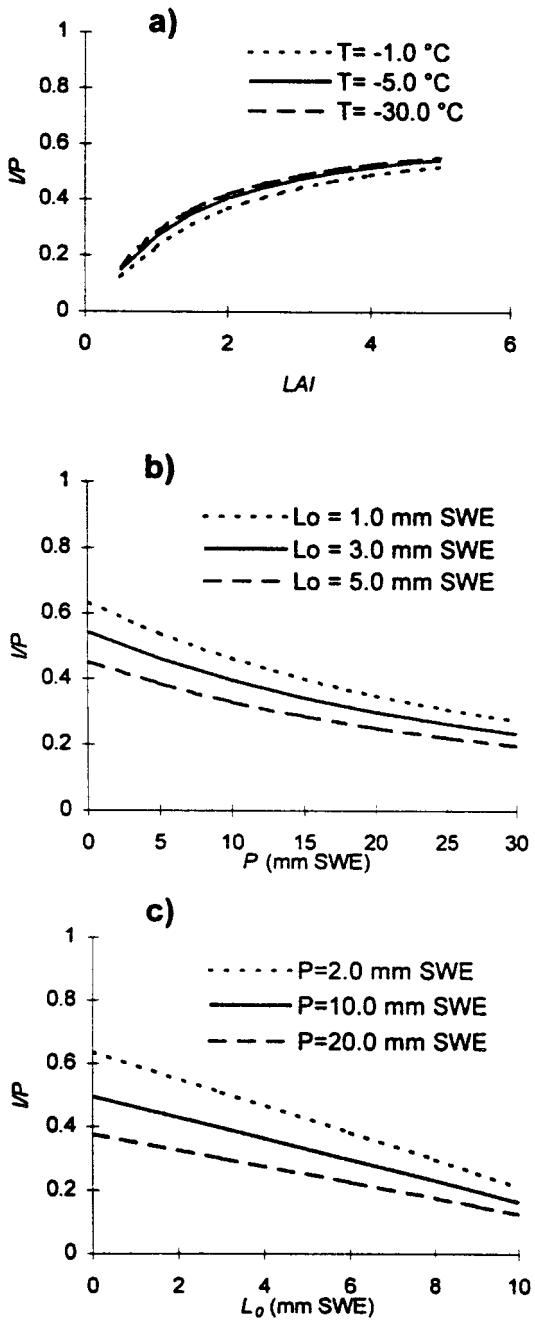

Figure 2. Performance of the process-based snow interception model for ranges of (a) leaf area index, (b) snowfall and (c) initial snow load

where Q_R is downwind blowing snow transport (kg/m/s) and Q_E is sublimation (kg/m/s). As evident from Equation (3), at the large spatial scales (fetches) of GCM grid cells, sublimation becomes the most important blowing snow flux, though transport strongly affects subgrid variability (smaller fetches) in snow accumulation. Reported annual fluxes of blowing snow sublimation range from 15% to over 40% (depending on climate, fetch and land use) of annual snowfall on the Canadian Prairies (Pomeroy *et al.*, 1993; Pomeroy and

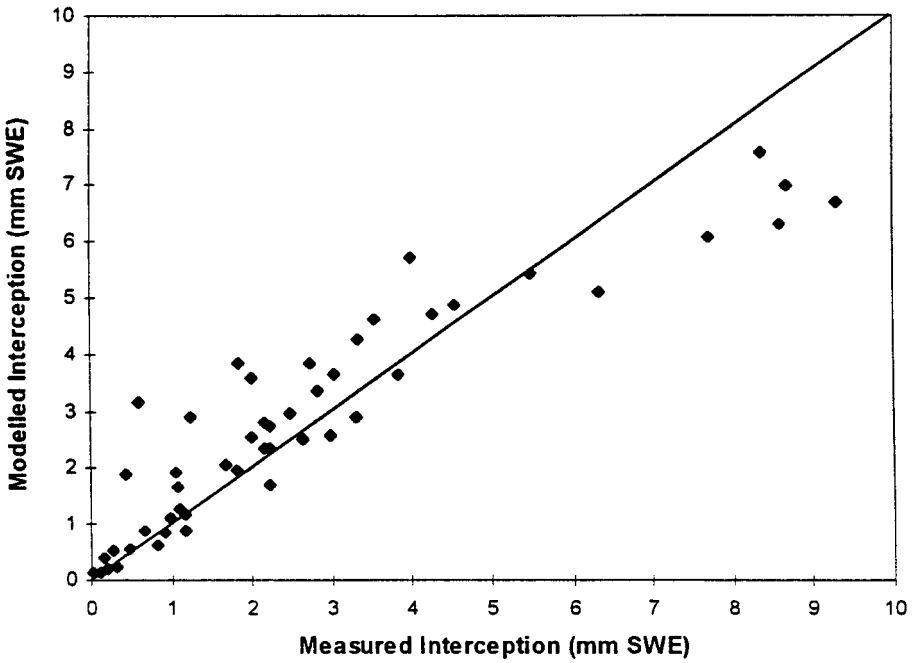

Figure 3. Measured and modelled snow interception. Comparison of the measurements from above and below canopy snowfall gauges, scaled-up using snow surveys and the results of the interception model for Beartrap Creek, 1993–1996

Gray, 1995), 28% of annual snowfall on tundra in the western Canadian Arctic (Pomeroy *et al.*, 1997b) and 32% of annual snowfall on the Alaska north slope (Benson, 1982). Blowing snow sublimation rates are higher than those expected for stationary snow because of the great exposure and ventilation that the snow crystals undergo when lifted by the wind and blown downfield (Dyunin, 1959; Schmidt, 1972; Pomeroy, 1989).

Land surface schemes do not incorporate blowing snow processes. This deficiency can result in appreciable errors in calculations of snow accumulation for open environments. For instance, in the Trail Valley Creek tundra basin in the western Canadian Arctic, Pomeroy *et al.* (1997b) measured an October–May snowfall of 190 mm SWE. The area is not subject to winter melting and has cold winter air temperatures with minimal surface snow evaporation. In May 1997, the maximum seasonal accumulations of snow water by landscape type were 68 mm on tundra, 252 mm on shrub tundra and 617 mm in drift areas (steep slopes). Similar magnitudes of difference between snow accumulation and snowfall are noted in the Canadian Prairies, though coupled blowing snow and snowmelt calculations are required to identify the causal factors because of the more variable winter climate of the region (Pomeroy and Li, 1997).

The Prairie Blowing Snow Model (PBSM) (Pomeroy, 1989; Pomeroy *et al.*, 1993) has been redeveloped for compatibility with GCMs, incorporating features for independent determination of the transport threshold for drifting (Li and Pomeroy, 1997a), upscaling blowing snow fluxes using probability theory (Li and Pomeroy, 1997b), improved vegetation parameterizations, simplified calculations for variable fetches and landscape-based snow mass balances that include snowmelt (Pomeroy *et al.*, 1997b; Pomeroy and Li, 1997). For instance, instantaneous blowing snow fluxes calculated for a point using a single-column, fetch-dependent calculation, Q_x, where x is either R or E, may be upscaled to a large uniform area such as a grid cell, g, using the probability of occurrence with respect to wind speed, u (m/s), which fits a cumulative normal distribution, as

$$Q_x(g) = \frac{Q_x}{\delta\sqrt{2\pi}} \int_0^u \mathrm{e}^{(\bar{u}-u)^2/2\delta^2}\, \mathrm{d}u \tag{4}$$

The parameters of the distribution, $\bar{u}$ and δ, are controlled by the air temperature, T (°C), and age of the snowpack, A (hours), where, following Li and Pomeroy (1997b)

$$\bar{u} = 11{\cdot}2 + 0{\cdot}365T + 0{\cdot}00706T^2 + 0{\cdot}9\ \ln(A) \tag{5}$$

and

$$\delta = 4{\cdot}3 + 0{\cdot}145T + 0{\cdot}00196T^2 \tag{6}$$

PBSM simulations for fallow and gully land surfaces, upscaled using this technique, along with the results of extensive landscape-based surveys for the Bad Lake Basin in 1974 are shown in Figure 4. The relative agreement between model and observations in both fallow field (transport out and sublimation dominated) and gully (transport in dominated) landscapes suggests that both the small-scale and large-scale snow mass balances can be simulated by a blowing snow model of this type (transport out of fallow must equal transport into gully and accumulation at either site must also balance any sublimation present). The seasonal sublimation and transport losses over the fallow field were 24 and 15% of annual snowfall, respectively, presuming a fetch of 1 km; had the fetch been 3 km the sublimation loss would have been 1·5 times this value, i.e. 36%. In the gully, the increases in snow accumulation owing to blowing snow transport ranged from 50 to 100% of cumulative snowfall. The data from the Arctic and Prairie environments illustrate the need to incorporate blowing snow routines into CLASS for more accurate grid- and subgrid-scale representations of seasonal snow accumulation and sublimation.

Snow densification

Snow density estimates are important for determining snow depth (when water equivalent is known), heat capacity, thermal conductivity and radiation extinction. Many land surface schemes either assume an average snow density of 250 kg/m^3 (e.g. UKMO, Essery, 1997) or calculate average snow density, assuming a density for fresh snow of 100 kg/m^3 and an exponential increase in density with time up to a maximum value (e.g. CLASS, Verseghy *et al.*, 1993; ISBA, Douville *et al.*, 1995). For these simulations appropriate initial snowfall densities, mechanisms for density increase after deposition and appropriate maximum snow densities are important.

Contrary to the assumption of constant new snowfall density equal to 100 kg/m^3, the average density of new fallen snow can vary widely, but for most parts of Canada it has been found to fall in a range between 50 and 120 kg/m^3. Lower values are found during cold, dry conditions and higher values are found in wet snow formed at warm temperatures (Pomeroy and Gray, 1995). Rather than a constant value, it is recommended that the algorithm developed by Hedstrom and Pomeroy (1998) be used to calculate the density of fresh snow, ρ_s(fresh), as a function of air temperature. This algorithm, which is based on extensive measurements by the US Army Corps of Engineers (1956) and Schmidt and Gluns (1991) is

$$\rho_s(\text{fresh}) = 67{\cdot}9 + 51{\cdot}3\ \mathrm{e}^{T/2{\cdot}6} \tag{7}$$

where T is the air temperature in °C. The algorithm provides for a rapid decrease in fresh snow density as temperature declines from 0 to −12 °C, and little further decrease for colder temperatures.

Following deposition, the density of new snow increases rapidly; however, the rate of increase depends on the *processes* causing the increase, e.g. crystal metamorphism in the snowpack, crystal settlement, melt and wind packing. Examples of density increases owing to wind packing and crystal settlement after wind packing show dramatic, episodic increases. Goodison *et al.* (1981) measured rates of snow density increase of 8–13 kg/m^3 h during snowstorms in Ontario (up to 12 h) and approximately 7 kg/m^3 h immediately after snowfall (up to 6 h) in conditions without blowing snow or melting. Gray *et al.* (1970) found that density for cold prairie snowpacks increased at approximately 9 kg/m^3 h during blowing snow storms (up to 24 h). For well-exposed snow in areas subject to snow storms and blowing snow it is appropriate to model episodic

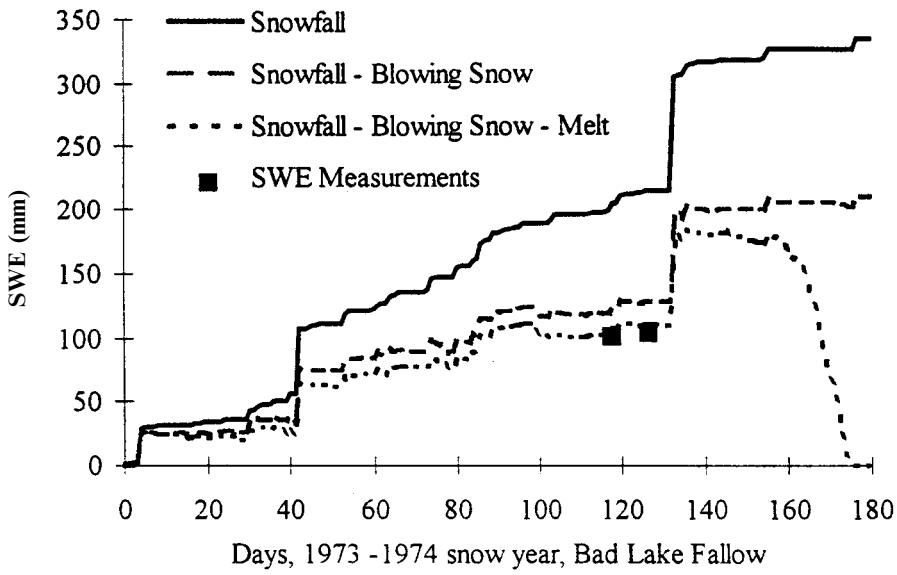

(a) Open fallow field, Bad Lake, SK, 1973-1974

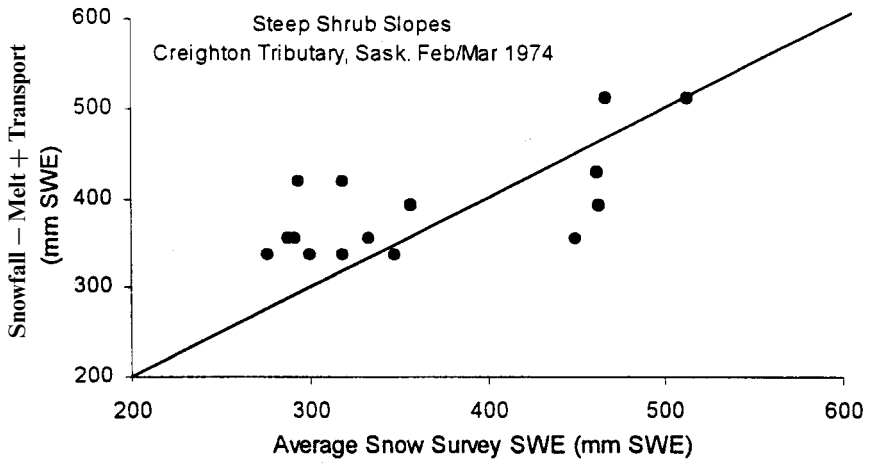

(b) Steep shrub-covered slopes, Creighton Watershed, SK, 1974.

Figure 4. Snow accumulation modelled for (a) open field of fallow at Bad Lake, SK, 1973–1974 and (b) steep shrub-covered slopes at Creighton Watershed, SK, 1974 using PBSM and SWE measured from extensive snow surveys

increases in density. For non-melting snow in open areas and hourly wind speeds greater than 7 m/s, it is recommended that snow density increase at a rate of 9 kg/m^3 h during the wind event, up to a maximum that is controlled by snow depth.

Various curves describing the seasonal increase in mean snow density in different environments are reported by Gray and Prowse (1993). These may be used to estimate the density increase due to metamorphism, which is the primary mechanism in cold, sheltered environments. For many sheltered environments (boreal forest, mountains), relatively slow density increases of the order of 25 kg/m^3 month are evident during the cold late-winter (February–March). Snowmelt causes rapid increases in apparent density (as

measured with a gravimetric device), with strong diurnal variation owing to inclusion of meltwater in pores of the solid phase of the snowpack. Melting snowpack densities range between 350 and 500 kg/m^3, with lower values in the morning and higher values later in the day as meltwater is generated as a snow cover is primed (Pomeroy and Gray, 1995).

The association between maximum cold snow density and depth has been examined in detail by Shook and Gray (1994) from 2400 measurements in the Canadian Prairies. For shallow, aged, wind-blown snow (mean depth, $d \leqslant 60$ cm), there is small covariance between depth and density and the mean density can be taken as 250 kg/m^3 (Shook and Gray, 1994). For deeper snow ($d > 60$ cm), there is a covariance between depth and density and the measurements of Shook and Gray can be used to modify an expression for density given by Tabler *et al.* (1990), which is based on extensive field measurements of the densities of snow drifts in Wyoming, USA. The form of the expression that matches density measurements on the Canadian Prairies is

$$\rho_s = 450 - \frac{20470}{d}[1 - e^{-d/67{\cdot}3}] \tag{8}$$

in which ρ_s is the mean snow density (kg/m^3) corresponding to mean snow depth (d, cm). Equation (8) gives the mean density for aged, seasonal, wind-blown snow, providing a maximum value for a non-melted snow cover in an open environment.

In forested and sheltered environments, the episodic density increase with snowfall is not apparent. However, dry snow densities for forested (boreal, mountain forest, maritime) environments with shallow snow (depth < 1 m) reach an approximate maximum value equal to 250 kg/m^3 (Gray and Prowse, 1993). Actual values will vary about this mean in response to metamorphism, which is sensitive to soil and air temperatures as well as snow depth. Equation (8) can be used to set a maximum snow density for deep mountain snowpacks that settle as a result of the weight of snow, since the derivation of the expression included observations taken in coastal mountain environments.

Spatial variation in water equivalent

The small-scale, spatial variation of the snow water equivalent (SWE) within a landscape type is well recognized, and before melt begins is due to wind redistribution of snow and the release of intercepted snow. Knowledge of this variation is especially important for calculating the snow-covered area at various stages of ablation, as explained in the next section of this paper. The spatial variation in SWE in forest environments is primarily a result of variations in winter leaf area (up to 70%, Pomeroy and Goodison, 1997) and proximity to individual trees (up to 40%, Woo and Steer, 1986; Jones, 1987; Sturm, 1992). In open environments, spatial variations in SWE are a result of wind exposure, topography and vegetation. Gray *et al.* (1979) show SWE on brush-covered hillslopes is over 10 times greater than that on bare soil hilltops in a prairie environment.

Table I lists representative, average values for the coefficient of variation (CV) of SWE that have been calculated from thousands of samples monitored in seasonal snow covers near the time of peak accumulation on various landscapes in prairie, arctic and boreal forest environments. The trends exhibited by these data are consistent with the findings reported in the literature (e.g. Woo and Marsh, 1977; Pomeroy *et al.*, 1997b) and field observations.

1. The variability in SWE on land with a taller vegetative cover is generally lower. Vegetation dampens the variability in water equivalent owing to landform. The denser the vegetation, the greater the effect. However, because of snow interception, evergreen forests produce a greater variability than do deciduous forests.
2. Snow accumulation patterns are affected by those topographic features that cause major divergence in air flow patterns, and therefore in snow erosion and deposition. This is evident in the larger values of the coefficient of variation for the crests of hills and the lee of abrupt slopes.

Table I. Representative values for the coefficient of variation of water equivalent of snow covers (CV) on various landscapes in prairie, arctic and boreal forest environments in late winter

Region	Land use and vegetation	Landform	CV
Prairies	Fallow	Flat plains; slightly to moderately rolling topography with gentle slopes	0·47
		Bottom (bed) of wide waterways; large sloughs and depressions	0·30
		Crests of hills, knolls, and ridges	0·58
	Stubble	All landforms	0·33
	Pasture	Flat plains; bottom (bed) of wide waterways; large sloughs and depressions; slightly to moderately rolling topography with gentle slopes	0·41
		Crests of hills, knolls, and ridges	0·51
		Lee of abrupt, sharp slopes	0·57
	Scattered brush	Bottom (bed) of waterways, e.g. gullies, sloughs and depressions	0·42
		Lee of abrupt sharp, slopes	0·52
	Treed farmyards		0·50
Arctic	Tundra	Flat plains, upland plateaux, slight to moderately rolling topography	0·31
		Valley bottoms	0·28
		Valley sides (drifts where slopes greater than 9°)	0·34
	Shrub tundra	Flat plains, slightly to moderately rolling topography	0·22
		Valley bottoms	0·16
		Valley sides (drifts where slopes greater than 9°)	0·18
	Sparse	Exposed hillside and forest edge	0·21
	Forest tundra	Sheltered	0·11
Boreal forest	Black spruce	All landforms	0·14
	Mature jack pine		0·10
	Mixed aspen–white spruce		0·05
	Young jack pine		0·14
	Recent clear-cut		0·07
	Recent burn		0·04

Estimates of CV determined by direct field measurement may vary appreciably around the values listed in Table I because:

(a) the landscape classification is qualitative and subjective;

(b) land use and landform features are not mutually independent;

(c) CV will vary with factors other than landscape features, e.g. with differences in processes affecting snow metamorphism, snowfall distribution, redistribution of snow by wind, interception and sample size. Many of the processes that cause redistribution affect the standard deviation and mean of SWE quite differently; and

(d) interannual changes in mean SWE associated with variable snowfall may alter the CV even with little change in processes that lead to the net redistribution flux.

SNOWMELT PROCESSES

The snowmelt period is one of rapid changes in land–atmosphere exchange since albedo, turbulent fluxes, internal snow energy and surface temperature undergo dramatic alteration as the snow cover becomes wet and is then depleted. Hydrology is also strongly affected since snowmelt water flows through the pack and

either infiltrates, evaporates or provides the spring freshet. In many northern environments the spring freshet is the largest annual runoff event, comprising approximately 50, 90 and 70% of annual flow for boreal forest, prairie and arctic environments, respectively (Gray, 1970; Hetherington, 1987; Woo, 1990). It is therefore critical for atmospheric and hydrological models to determine properly areal energy fluxes, radiative and turbulent exchange with the snowpack, internal energy changes and energy exchange with the ground during the melt period. This section examines the change in snow-covered area during melt and melt energetics.

Snow cover depletion

Most snow covers disintegrate into a mosaic of patches of snow and 'bare' ground as they ablate. This disintegration affects the geometry and area of snow cover, which affects the energetics of the melt process and the contributing areas of melt, runoff, infiltration and soil water recharge. In order to include the effects of the patchiness of a snow cover on these components in snowmelt simulations it is necessary to incorporate in the algorithm a measure of the geometrical character of the snow field during ablation. Most land surface algorithms do not consider the decrease in snow-covered area during snowmelt. CLASS, however, does when the mean depth of snow is $\leqslant 10$ cm, the limiting snow depth after which bare patches begin to appear (Donald *et al.*, 1995). It calculates snowmelt as the volume of meltwater produced per unit area of grid cell. This quantity, M, the resultant melt, is the *result* of the application of M_a, applied melt, that melt per unit area of snow which occurs over snow. Therefore, the fraction of snow cover, F_s must be known to calculate M from M_a. The two quantities are related by

$$M = \int_0^{M_a} F_s \, dM_a \tag{9}$$

where the areal fraction of snow cover, F_s is

$$F_s = \frac{W_s}{0{\cdot}10\rho_s} \tag{10}$$

in which W_s is the mass of snow per unit over the grid (kg/m^2) and ρ_s is the snow density (kg/m^3).

Two assumptions used by Equation (10) conflict with the spatial statistics of most natural ablating snow fields. They are:

(a) areal snow cover depletion starts when the mean snow depth is equal to 10 cm, and

(b) the spatial distribution of snow water is uniform.

Shook (1993, 1995) and Shook *et al.* (1993, 1994) demonstrated that in environments where the melt flux is relatively uniform over an area, the fractal character of the spatial distribution of the water equivalent controls the geometries of the soil and snow patches of an ablating snow cover.

Donald *et al.* (1995) also showed clearly the snow depth distribution for snowpacks in southern Ontario followed a three-parameter log–normal distribution. Once the limiting snow depth was reached, the depth distribution followed a two-parameter log–normal probability density function. Using this function, Donald (1992) derived a simple 'melt model' where the theoretical average snow depth and fraction of snow (F_s) curves could be described through a uniform downward shift (applied snowmelt, M_a) of the depth distribution. The remaining snow-covered area fraction, F_s, is given by (Donald *et al.*, 1995)

$$F_s(M_a) = \frac{1}{2} erfc(z_{M_a}/\sqrt{2}) \tag{11}$$

where

$$z_{M_a} = \left(\frac{\ln M_a - \lambda}{\xi}\right);\ \xi = \sqrt{\ln(1 + \sigma^2/\mu^2)};\ \lambda = \ln(\mu) - \frac{1}{2}\xi^2$$

where μ and σ are the mean and the standard deviation of the snow depth at the limiting value and *erfc* is an error function. Note that the definition of λ corrects an error in the paper by Donald *et al.* (1995). The corresponding expression for the average snow depth over the entire grid cell area, $\bar{D}$, resulting from the same distribution shift of M_a was solved analytically as (Donald *et al.*, 1995)

$$\bar{D}(M_a) = \frac{1}{2}e^{\mu+1/2\xi^2} erfc\left[\frac{1}{\sqrt{2}}(z_{M_a} - \xi)\right] - M_a F_s(M_a) \tag{12}$$

Shook (1995) noted that the spatial frequency distribution of the snow water equivalent (SWE), as opposed to snow depth, of a natural snow cover can often be approximated by the log–normal probability density function, which he expressed in linear form as

$$SWE = \overline{SWE}(1 + K\ CV) \tag{13}$$

where the terms are: *SWE*, snow water equivalent having an exceedance probability equal to that of the frequency factor, *K* [see Chow (1954) for calculation procedure]; $\overline{SWE}$, mean snow water equivalent; and *CV*, coefficient of variation. Figure 5 plots point measurements of SWE and fitted log–normal distributions for three landscapes in a prairie environment for (a) a relatively flat field in wheat stubble, (b) an undulating field of fallow and (c) a relatively flat low area with scattered brush. The respective coefficients of determination (r^2) between the measured and fitted SWE values for the landscapes are 0·92, 0·98 and 0·99, respectively.

Shook (1995) also noted that the snow cover depletion curve is produced by applying the snowmelt rate evenly over the SWE frequency distribution. The applied snowmelt is designated M_a and represents the total amount of snow melted at any point in the snow cover. If there is no covariance between depth and density of snowpacks (as is the case for shallow snow) then the algorithm of Donald *et al.* (1995) can be applied without modification and applied melt is equivalent to the shift in the snow depth distribution, M_a. Therefore, under conditions where the melt flux over an area is approximately uniform, a reasonable representation of the

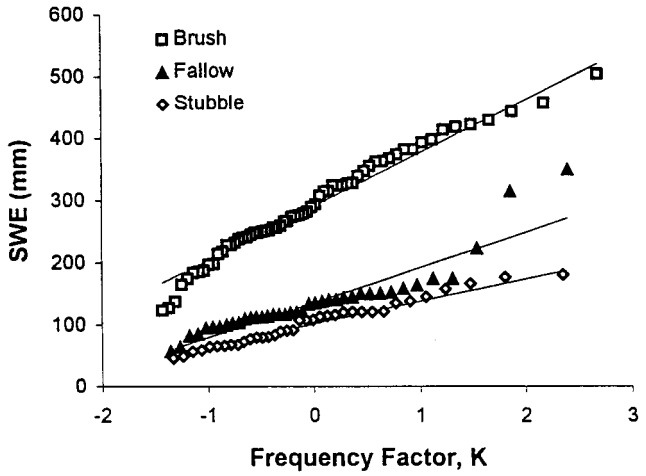

Figure 5. Log–normal distribution fitted to point measurements of SWE taken on open landscapes in brush, fallow and wheat-stubble — Smith Tributary, SK, 1972

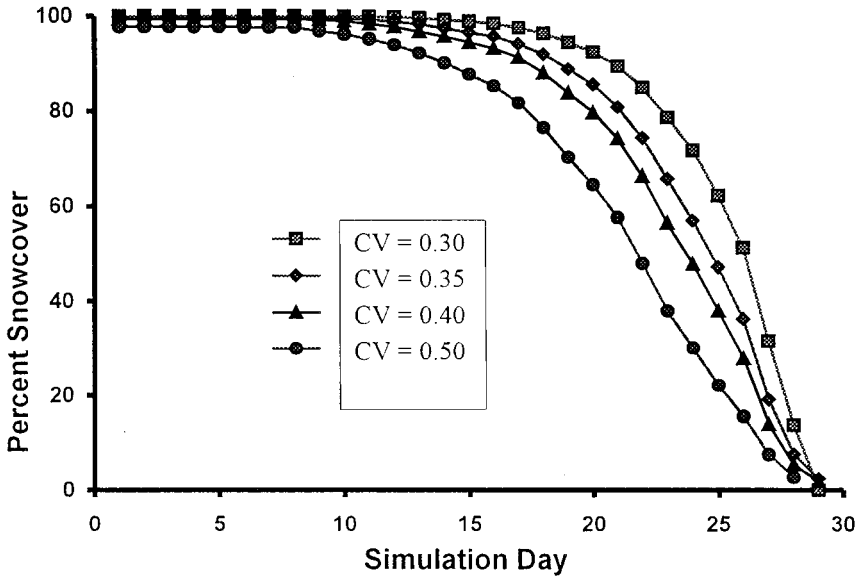

Figure 6. Snow-covered area depletion curves modelled by applying a constant, uniform melt rate to snow covers whose SWE have a log–normal distribution. Fractional snow cover is plotted against time from an initial SWE of 130 mm for various coefficients of variation of SWE, CV

depletion of snow-covered area (F_s) during ablation can be obtained by melting the frequency distribution of SWE or solving directly using Equations (11) and (12).

The results of this procedure are demonstrated in Figure 6, which plots the decrease in F_s over time for a constant melt rate, assuming initial conditions of a log–normal distribution of SWE with various CV values. The results show that the smaller the CV, the more rapid the depletion of F_s. This trend is the result of the increased peakedness of the frequency distribution of SWE with decreasing CV. The smaller the CV, the larger the number of SWE values grouped near to the mean.

The snow-covered area depletion algorithm developed by Shook (1995) was tested using data collected on the Smith Tributary at Bad Lake in 1972, with melt rates driven by a temperature-index model. The results are shown in Figure 7 and demonstrate reasonable correspondence between modelled and measured areal depletion of snow cover (Shook, 1995).

Snowmelt energetics

Land surface schemes calculate the energy available for snowmelt (Q_m) by an energy balance equation. Therefore, assuming a continuous snow cover

$$Q_m + Q_n + Q_h + Q_e + Q_a + Q_g = dU/dt \tag{14}$$

The terms of Equation (14) are Q_n, net radiation; Q_h, turbulent flux of sensible heat exchanged at the surface due to a difference in temperature between the surface and overlying air; Q_e, turbulent flux of latent energy exchanged at the surface due to vapour movement as a result of a difference in vapour pressure between the surface and overlying air; Q_a, energy advected to the snowpack from rainfall or other processes; Q_g, ground heat flux due to conduction; U, internal energy; and t, time. With the exception of Q_a and dU/dt, the various terms in Equation (14) are examined below with respect to measurements, land surface scheme representations and process algorithms. Discussions of the Q_a term have been recently provided by Liston (1995), Shook (1995) and Marsh *et al.* (1997), whilst Male (1980) and Marsh and Woo (1984) provided a detailed examination of dU/dt.

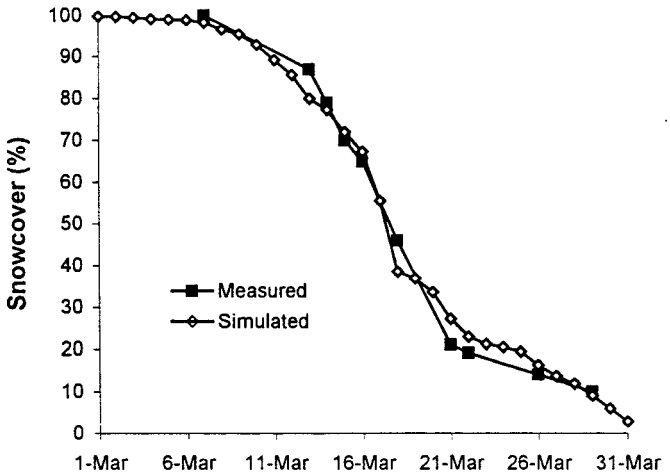

Figure 7. Modelled and measured snow cover depletion curves during snow ablation on the Smith Tributary in 1972

Radiation. The radiation balance in land surface schemes is typically composed of long- and short-wave terms. The long-wave balance as affected by snow depends on the surface temperature, which is normally solved for by an iterative solution of an energy balance at the surface. Actively melting snow has a surface temperature of 0 °C; departures from this value at night depend on snowpack internal and external energetics. Errors in other components of the energy balance can therefore cause errors in the long-wave flux.

Short-wave energy fluxes are influenced by the snow albedo. The interaction between vegetation and snow cover albedo is complex however, even when snow covers vegetation. For instance, Pomeroy and Dion (1996) have shown that snow-covered boreal pine canopies act as 'light-traps', such that the canopy albedo is unaffected by intercepted snow load. Some land surface schemes correctly simulate this feature (CLASS, SiB, UKMO) but some increase canopy albedo after recent snowfalls (ECMWF, Betts *et al.*, 1996). In shrub-covered clearings of the boreal forest, Pomeroy and Granger (1997) found net radiation during melt became enhanced as low shrub vegetation became exposed, lowering the albedo. For this reason, $Q_n - Q_g$ was 2·36 times Q_m over the melt period and turbulent contributions to melt were negligible. For surface snow covers, most land surface schemes neglect the role of protruding vegetation, but some do reduce the albedo as fresh snow ages, with further modifications during melt (e.g. ISBA, MPI, CLASS). For instance, CLASS assumes an albedo for 'fresh' snow of 0·84 to a lower limit of 0·70 for 'old snow'. The variation in snow albedo, α_{sn}, with time, t(s), is approximated by the expression

$$\alpha_{sn}(t+1) = [\alpha_{sn}(t) - 0{\cdot}70] \exp\left(\frac{-0{\cdot}01\Delta t}{3600}\right) + 0{\cdot}70 \tag{15}$$

α_{sn} decreases until a new snowfall event occurs, which returns the albedo to 0·84. The lower limit of 0·7 is decreased further to 0·50 if liquid water is present on top of the snowpack (Verseghy *et al.*, 1993).

Modelling studies such as that by Wiscombe and Warren (1980) provide the albedo of complete snow covers from theoretical principles and have been successfully incorporated in snow models (Marshall and Oglesby, 1994). However, it is often difficult to interpret field measurements of areal albedo (α) made with hemispherical radiometers because of the decrease in snow-covered area during melt. Field measurements of albedo can be corrected using measured fractions of snow-covered area (F_s) from aerial photographs to provide estimates of the variation of α_{sn} during melt. For patchy snow cover, the snow albedo (α_{sn}) is obtained from areal albedo by weighting the albedos of the snow and the ground according to a segregation

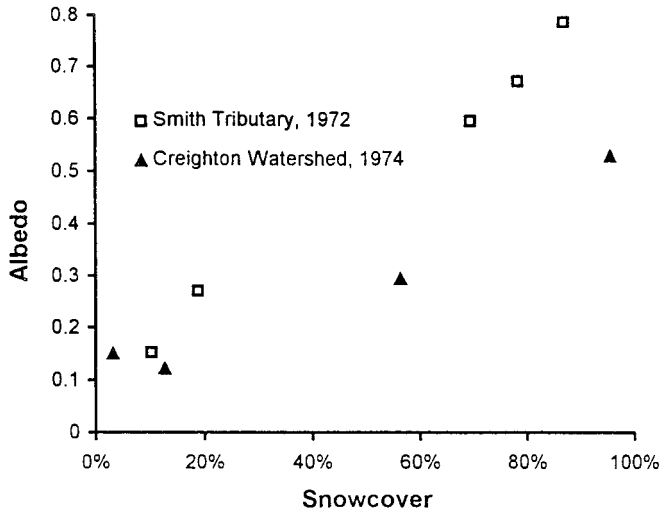

Figure 8. Relationship between areal albedo, α, and snow-covered area, monitored on two small watersheds at Bad Lake, SK

based on the fraction of the unit area covered by each surface. This technique is commonly employed by recent land surface schemes to calculate areal albedo during melt, and is

$$\alpha = \alpha_{sn} F_s + \alpha_g (1 - F_s) \tag{16}$$

where α_g is the albedo of snow-free ground.

Using aerial photographs, and aerial and point albedo measurements, Shook (1993) demonstrated that the association between α and F_s during snowmelt on the Canadian Prairies is approximately linear over a large range in F_s (0·9–0·1), as shown in Figure 8. A linear association between α and F_s suggests that α_{sn} does not vary greatly during ablation and that the major factor controlling the decay in α is the fraction of bare ground. The upper limit of α is established primarily by α_{sn}, closely following the start of depletion in F_s; the lower limit is set by α_g. Fitting a linear regression to the data for Smith Tributary, Bad Lake, Saskatchewan in Figure 8 gives an intercept of 0·096 and a slope of 0·75, with a correlation coefficient, $r = 0{\cdot}99$. The corresponding values for the albedos of ground and snow by Equation (16) are therefore $\alpha_g = 0{\cdot}096$ and $\alpha_{sn} = 0{\cdot}85$. A similar analysis applied to the measurements for the Creighton sub-basin of Bad Lake gave the corresponding statistics: intercept = 0·095, slope = 0·42, $r = 0{\cdot}95$, $\alpha_g = 0{\cdot}095$ and $\alpha_{sn} = 0{\cdot}52$. The lower albedo for snow on the Creighton Watershed is due to a shallow, dirty snow cover and vegetation protruding through the snow surface. The large differences in snow albedo between snow covers of similar grain size and wetness suggest that much of the variation in albedo with grain size may be overwhelmed by local factors such as dust, pollution and protruding vegetation. These results also suggest that the changes in the reflectance of snow during ablation are small and have little effect on α. The data call into question the presumption in albedo calculations that melting snow is 'clean' and covers vegetation during melt. The decrease of α_{sn} to 0·5 for wet snow by CLASS would also appear inappropriate as the field measurements provided no evidence that snow albedo declines during the decrease in snow-covered area. It would satisfy the trends shown in measured data to simply fix the snow albedo, determined at the beginning of the snow-covered area depletion, throughout subsequent melt, and account for the change in areal albedo by the progressive exposure of bare ground and vegetation during melt.

Ground heat flux. Most simulations of ground heat in land surface models are based on heat transfer by conduction using the temperature gradient approach and simulated soil temperatures at 3 or 4 levels in a soil profile that extends to the rooting depth of the crop or below. Often, heat transfers resulting from phase

changes from freezing and thawing in frozen soils are either ignored or the freezing point depression relationship — the curve describing the association between liquid water content and freezing temperature — is represented as a step function rather than as a continuous curve.

When water from a melting snow cover is unable to infiltrate a frozen soil, such as may occur when an ice lens has formed on the soil surface or in ice-rich, uncracked permafrost, the temperature gradient method may be expected to give reasonable estimates of the ground heat flux. If the soils are very cold, intense temperature gradients and high fluxes may develop and lead to the formation of basal ice layers at the soil surface (Woo *et al.*, 1982). The refreezing may result in large changes in the internal energy of the snowpack (Marsh and Woo, 1984).

For most northern regions, however some infiltration of meltwater into frozen soils accompanies snow ablation. Under these conditions the ground heat flux is usually small compared with the melt energy flux. Average daily ground heat fluxes generally fall in the range from 0 to 4·6 W/m^2. Nevertheless, where algorithms are used to estimate the flux, the component must be calculated correctly because a large error in the calculation may affect the determination of the other terms of the energy equation and closure of the energy balance. For example, a poor estimate of snow surface temperature will affect the calculations of albedo, sensible and latent heat in most land surface models.

The application of a temperature gradient approach for estimating the ground heat flux in frozen soils during snowmelt infiltration is often not appropriate. A major reason for the difficulty is that important heat and mass transfer processes affecting the flux occur in the upper portion of the soil temperature profile. For example, Gray *et al.* (1985) reported that the average depth of meltwater penetrating frozen agricultural soils of the Canadian Prairies was about 30 cm (standard deviation = ±10 cm).

Infiltration into frozen ground involves simultaneous coupled heat and mass transfers with phase changes. Field measurements (Kane and Stein, 1983) and model simulations (Zhao *et al.*, 1997) demonstrate that both the infiltration rate and the surface heat transfer rate (conduction) decrease with time following the application of meltwater to the surface (Figure 9). Zhao *et al.* (1997) suggested that these variations may be described by two regimes, a transient regime and a quasi-steady-state regime. The transient regime follows immediately on the application of water to the soil surface. During this period the infiltration rate and the heat transfer rate decrease rapidly. The quasi-steady-state regime develops when the changes in the infiltration rate and the heat transfer rate with time become relatively small. The duration of the transient period is usually short (a few hours), depending on the hydraulic properties of the soil, surface conditions, initial water content and initial temperature of the soil. During transient flow, the energy used to increase the

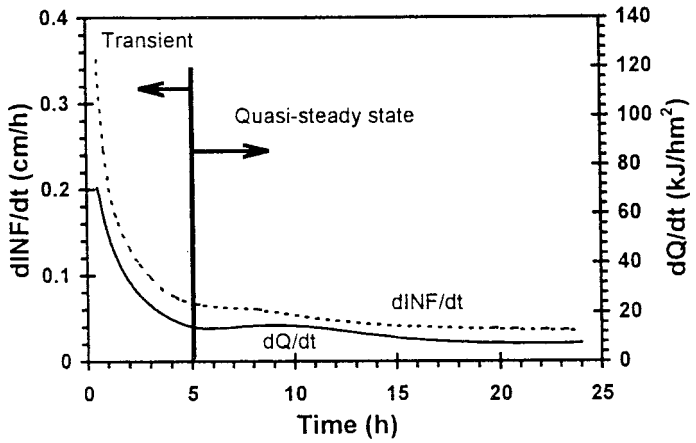

Figure 9. Variations in infiltration rate (d*INF*/d*t*) and surface heat flux rate (d*Q*/d*t*) with time during snowmelt infiltration into a frozen silty clay soil

soil temperature is largely supplied by heat conduction at the surface (high heat transfer rate at the surface) (Zhao *et al.*, 1997). In the quasi-steady-state regime, the energy used to increase the soil temperature at depth is supplied by latent heat released by the refreezing of percolating meltwater in the soil layers above (low heat transfer rate at the surface).

Figure 10 shows simulated profiles of ice content, θ_i (Figure 10a), heat flux, dQ/dt (Figure 10b) and soil temperature, T (Figure 10c) after 2, 8, 12 and 24 h of infiltration into a frozen soil with initial and boundary

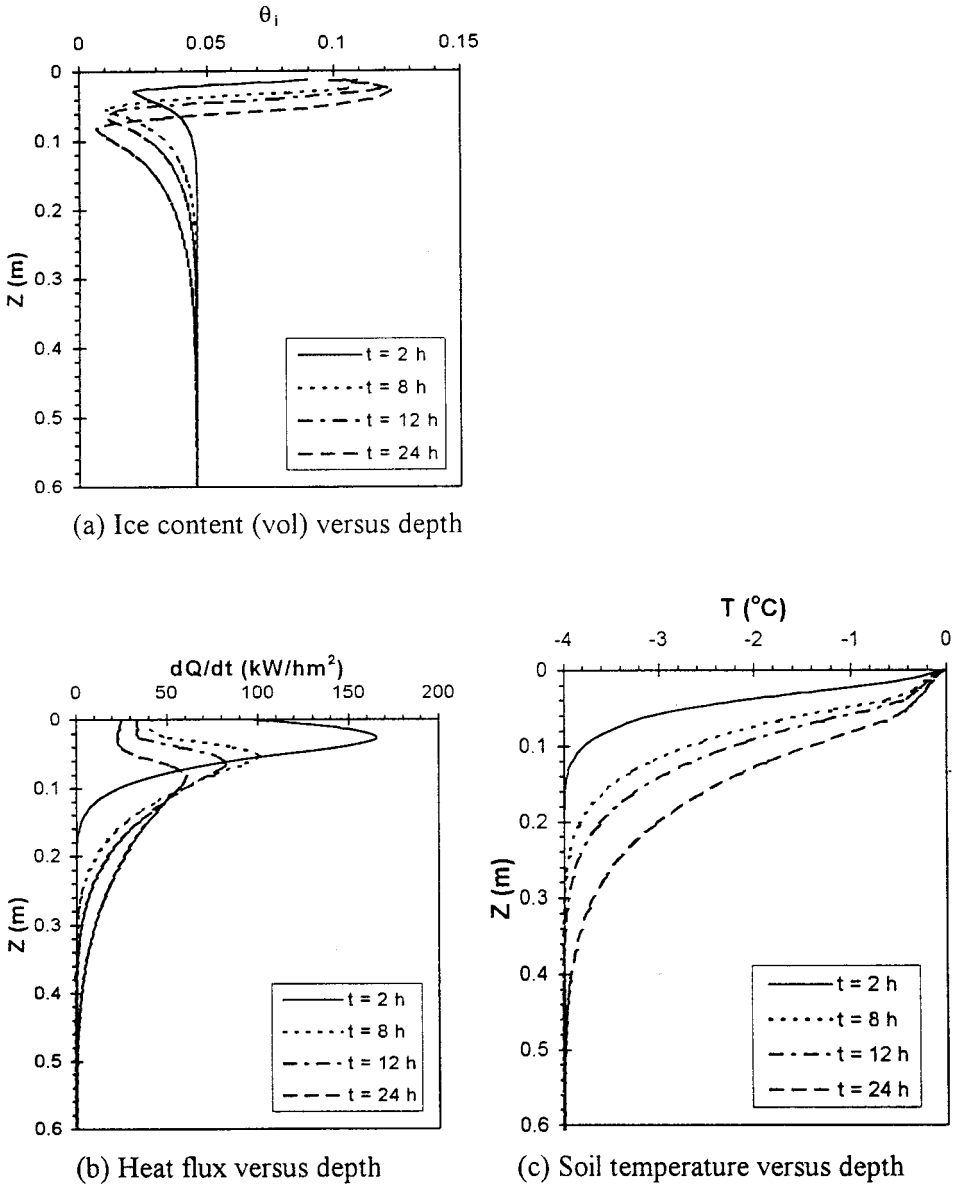

Figure 10. Simulated profiles of variations in: (a) ice content, (b) heat flux and (c) soil temperature with depth after 2, 8, 12 and 24 h of continuous snowmelt infiltration into a frozen silty clay soil. Initial and boundary conditions: soil pore saturation = 0·40, surface pore saturation = 0·75 and soil temperature = −4 °C

conditions of: total soil moisture pore saturation = 0·40, soil temperature = −4 °C and surface pore saturation = 0·75. The snowpack in contact with the soil is at the melting point with a constant melt rate. Figure 10a shows soil layers with an increase in ice content (freezing) overlying soil layers with a decrease in ice content. Most of the latent heat (say 90%) released by the refreezing of meltwater is conducted deeper in the soil, where it is used for melting and increasing the soil temperature (Zhao *et al*., 1997). Figure 10b shows that the depth of maximum heat flux coincides with the depth of maximum melting (Figure 10c). The heat flux dampens as the maximum flux moves deeper into the soil. As indicated above, the energy added to a soil by conduction from the surface is only important to the thermal balance during the early stages of infiltration. With increasing time the ground heat flux decreases because of decreases in the temperature gradient in soil layers near the surface (Figure 10c). Until such time as these simulations or representations of such can be included in land surface models, ground heat flux calculations in GCMs should be capped to remain small during infiltration into frozen soils.

Turbulent fluxes. The success of determining the melt flux over snow by Equation (14) can be highly variable, which is often attributed (see Male and Granger, 1979) to the difficulties in obtaining accurate, reliable estimates of the convective turbulent fluxes by bulk aerodynamic transfer equations similar to those used in many land surface schemes. Land surface models parameterize exchanges of heat and moisture between the atmosphere and the surface using relationships of the form

$$Q_h = \rho_a C_p D_h u \Delta T \tag{17}$$

and

$$Q_e = \rho_a h_v D_e u \Delta q \tag{18}$$

where ρ_a and C_p are the density and heat capacity of air, h_v is the latent heat of vaporization, D_h and D_e are exchange coefficients, u is the wind speed at a reference height in the atmosphere, and ΔT and Δq are temperature and humidity differences between the surface and the reference level. The surface humidity is generally assumed to be saturated over snow and the surface temperature cannot rise above 0 °C; snowmelt is diagnosed from the energy required to balance the surface energy budget subject to the surface temperature constraint. Exchange coefficients are calculated as functions of surface roughness and some index of atmospheric stability — either a Monin–Obukhov length or a Richardson number.

Those factors contributing to the difficulties and problems in calculating turbulent exchange in this manner include:

1. The validity of the assumption of a constant flux layer. de La Casinière (1974), Granger (1977) and Halberstram and Schieldge (1981) observed a temperature maximum in the air layer 10–50 cm above the surface of melting snow owing to radiation heating. With the upper limit of the snow surface temperature at 0 °C, this temperature anomaly results in a shallow, stable profile directing heat towards the surface. When upper air temperatures are less than this maximum, not only is the heat flux not constant with height but it may undergo a reversal in direction at the level of the raised maximum. Expressions that make use of the air temperature at 1–2 m and the temperature of the snow surface can therefore give a sensible heat flux in the wrong direction.

2. Typically, snow covers have low thermal conductivities and high albedos and emissivities and a snow surface can be very cold, especially on cold nights. This results in extremely stable conditions of the atmospheric surface layer, which dampen turbulent mixing (Male, 1980).

3. The eddy diffusivities for latent and sensible energy and momentum are not equal (Male and Granger, 1979).

Table II. RMS errors (W/m^2) during isothermal melt of a continuous open snow cover in estimates of snowmelt heat fluxes by various commonly used turbulent exchange algorithms, compared with net radiation less ground heat flux. Kernen Farm, Saskatoon, 1996

	Webb	Granger	McFarlane	$Q_n + Q_g$
11 March	10·0	10·0	13·0	2·8
12 March	10·7	9·0	13·0	2·0

4. Snow and ice are smooth surfaces that lead to low shear velocities and low induced levels of turbulence. Yen (1995) estimated the sensible heat flux over snow- or ice-covered ground during the winter months as only about one-third of that over grass-covered ground during the spring and summer months.

A comparison of turbulent flux schemes during snowmelt was made for an isothermal, continuous, unvegetated snowpack near Saskatoon on 11 and 12 March 1996, and is shown in Figure 11. Three schemes were tested: the 'log-linear' form commonly used for stable conditions (Webb, 1970), a modification developed by Granger and Male (1978) from measurements over snow and a Richardson number formulation typical of the type used in large-scale atmospheric models (McFarlane *et al*., 1992). For comparison, net radiation less ground heat flux is shown. *All* of the turbulent transfer schemes overestimate the downward (largely sensible) convective energy available for melt, the degree of overestimation depending upon the stability correction employed by the scheme. RMS errors in estimates of snowmelt heat fluxes over the 13:00–17:00 period are shown in Table II for both days. Interestingly, the 'best' melt rate simulation is obtained by disabling the turbulent transfer schemes and simply using net radiation and ground heat flux to estimate snowmelt.

Model simulations of melt

An appreciation of the difficulties of modelling snowmelt with even a relatively sophisticated land surface scheme, and the limited degree of improvement in performance that can be expected when correcting algorithms of a scheme in isolation, is shown in the following section, with respect to CLASS. CLASS was chosen because it contains representations of the phenomena demonstrated (snow-covered area depletion, energetics of snowmelt, multi-layer soil model) and should be expected to perform well in a major Canadian environment (prairies).

Snow-covered area depletion. An attempt was made to examine the effect of incorporating the recommended snow cover depletion curve in CLASS on performance during ablation on a flat unvegetated field near Saskatoon in 1994 (Figure 12). The comparisons show that both CLASS and modified CLASS (with the snow cover depletion algorithm) are about 5 days late in the prediction of the start of snow cover depletion compared with that measured. The delay, caused by various unknown errors, makes it impossible to assess changes in performance owing to the new snow cover depletion curve. This observation also suggests that the benefits of more physically realistic snow-covered area depletion cannot be realised without an assessment of the energetics of the CLASS snowmelt routine.

Snowmelt energetics. Energy flux measurements collected near Saskatoon during 11–13 March 1996 were used to examine the performance of CLASS simulations of the melt of shallow, continuous, open environment snow covers. CLASS was run on an hourly basis using net long-wave and incoming short-wave radiation, air temperature, wind speed and dew point. Initial snow and soil conditions were determined by field measurements. Figure 13 compares the 30-minute melt fluxes calculated by CLASS with those calculated using measured components in the energy equation [Equation (14)] on 12 March 1996 near Saskatoon. CLASS tends to underestimate the net energy available for melt, with values ranging from 50 to 64 W/m^2 during periods in the afternoon, and averaging 35 W/m^2 over the interval 12:30–17:00. Another

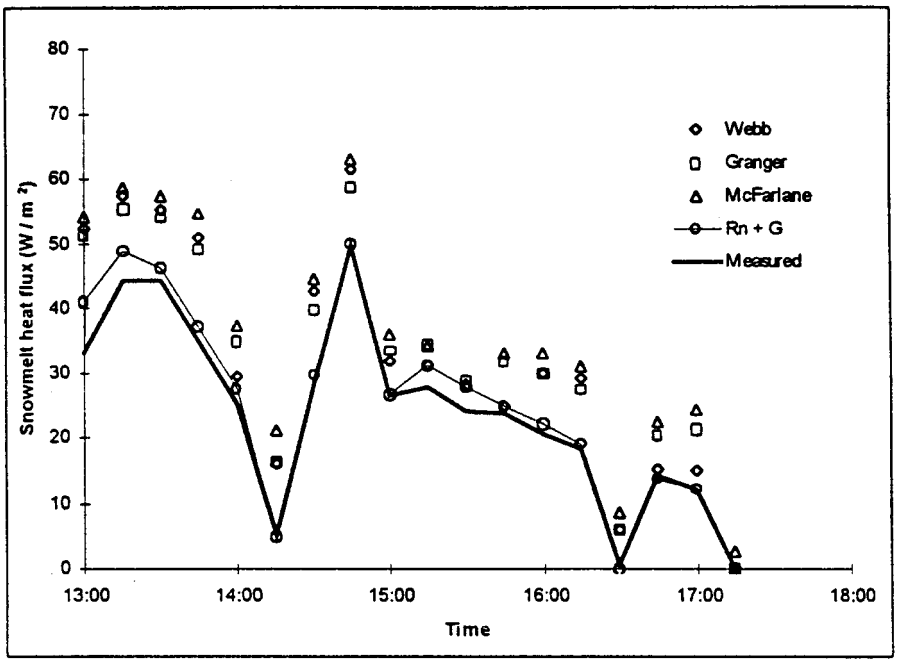

a) 11 March 1996

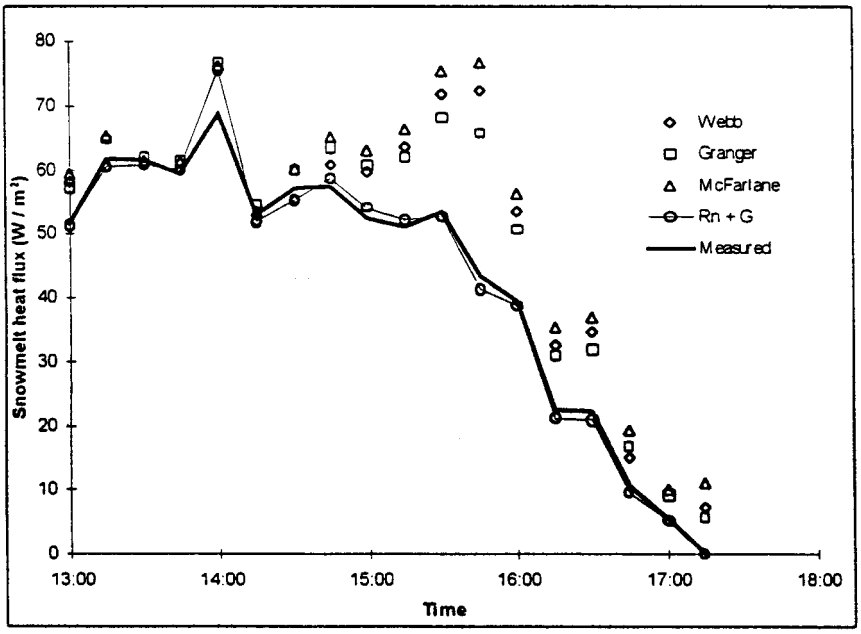

b) 12 March 1996

Figure 11. Comparison of snowmelt heat flux measured using the measured inputs to the energy balance equation, and modelled using ground and radiation fluxes and estimated sensible and latent heat fluxes from the following schemes: Webb (1970), Granger and Male (1981) and McFarlane *et al.* (1992). The net radiation less ground heat flux is shown for further evaluation of the actual contribution from turbulent fluxes

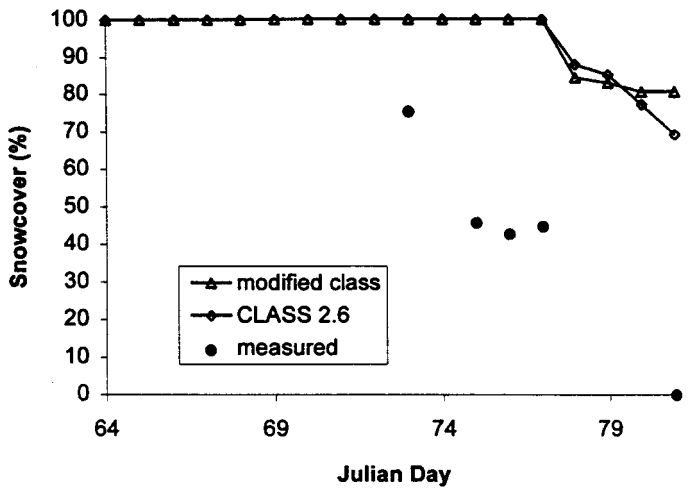

Figure 12. Comparison of CLASS and modified CLASS in predicting snow cover depletion on a flat field of fallow at Kernen Farm, near Saskatoon, March 1994

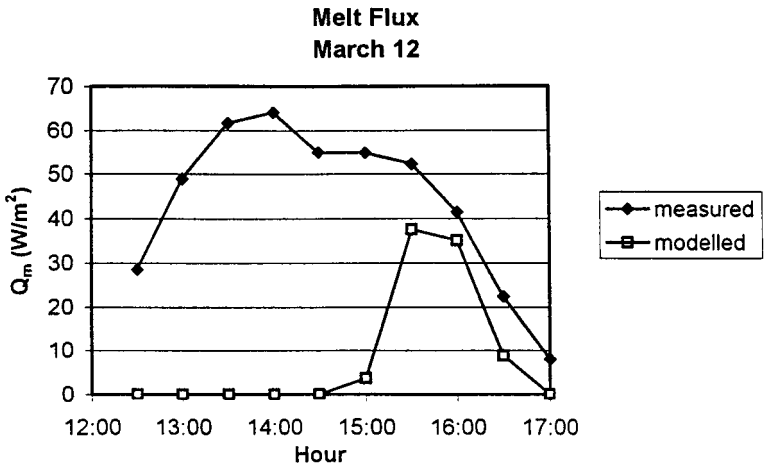

Figure 13. Comparison of 30-minute melt fluxes calculated by CLASS, and corresponding values determined using measured components in the energy equation, Kernen Farm, near Saskatoon, 12 March 1996

important feature demonstrated in Figure 13 is the delay in timing of melt by CLASS. CLASS does not show melt occurring until 15:00.

To study the effects of deviations in the modelled estimates of components of the energy equation on the calculation of the melt flux, comparisons between 'modelled' and 'measured' values were made for the three-day period on the Kernen Farm when the measured melt fluxes (determined using measured values in the energy equation) were positive. Figure 14 plots 'modelled' versus 'measured' 30-minute fluxes for: (a) net radiation, (b) latent energy, (c) sensible energy and (d) ground heat for the same time period on 12 March 1996 described by Figure 13. The data in Figure 14a show good agreement between 'modelled' and 'measured' net radiation, with a trend for CLASS estimates to be slightly higher than the measurements. For the three-day period, the variables showed strong correlation, with a coefficient of determination $r^2 = 0{\cdot}99$, a mean difference ('modelled' – 'measured') equal to $4{\cdot}28$ W/m^2 and a standard deviation of the differences

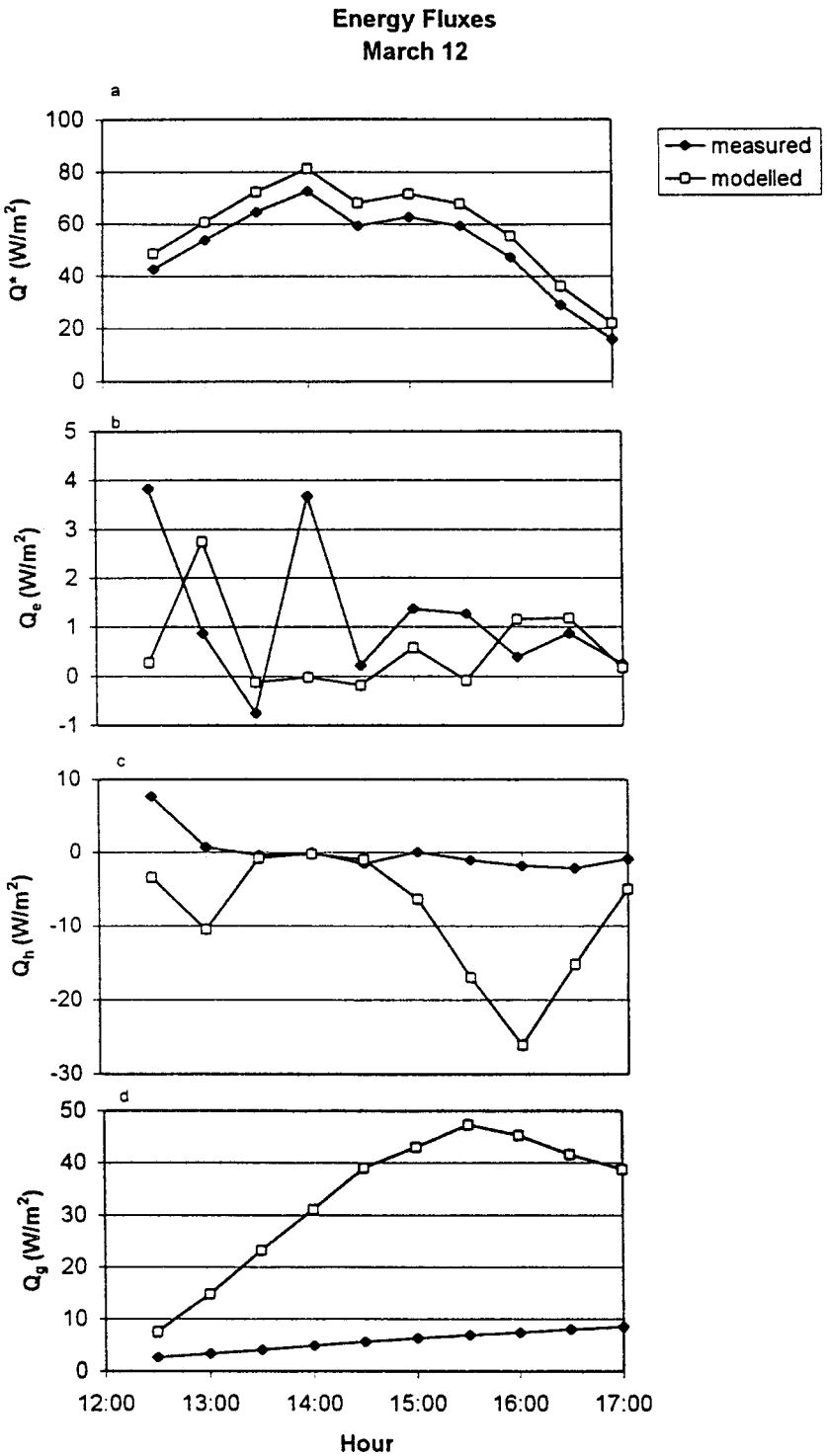

Figure 14. Comparisons of CLASS-modelled and measured 30-minute fluxes at Kernen Farm, near Saskatoon, during melt on 12 March 1996: (a) net radiation, (b) latent energy, (c) sensible energy and (d) ground heat. Note net radiation is positive when directed to the pack, all other fluxes are positive when they are directed away from the pack

equal to 3·43 W/m^2 (see Figure 15a). The difference is largest for high values of net radiation and may be presumed to be due to CLASS underestimating snow albedo.

Figure 14b shows poorer association between the 'modelled' and 'measured' latent energy, compared with net radiation, but with no strong systematic trend for the CLASS values to either overestimate or underestimate the measurements. A closer inspection of the association of the latent fluxes is provided in the scatter diagram of these fluxes for the three-day period in Figure 15b. The association has an r^2 of 0·74, with a mean different equal to 2·48 W/m^2 and standard deviation of the difference equal to 6·94 W/m^2. The largest relative deviations (10–15 W/m^2) are associated with the largest latent heat fluxes (positive or negative). In other words there is a general trend for CLASS to overestimate the measured values slightly, with the degree of overestimation increasing with the magnitude of the latent heat.

Figure 14c shows wide variations between 'modelled' and 'measured' sensible energy on 12 March 1996 with small deviations during the middle parts of the period, and reaching about -23 W/m^2 when meltwater is generated (see Figure 13). A scatter diagram of 'modelled' versus 'measured' sensible energy fluxes during the three-day period is shown in Figure 15c. Deviations are largest when measured sensible heat is nearly 0, but the modelled sensible heat ranges from $+2$ to -28 W/m^2. The association between values has an r^2 of 0·27, with a mean difference of $-4·48$ W/m^2 and a standard deviation of differences equal to 8·34 W/m^2.

Figure 14d shows that the CLASS estimates of the ground heat flux are consistently much higher than the corresponding measured value. Over the three-day period the association between variables was $r^2 = 0·34$, with a mean difference of 11·40 W/m^2 and standard deviation of differences equal to 14·94 W/m^2 (Figure 15d). On 12 March, the overestimation of the ground heat loss by CLASS contributed 78·2% of the shortfall in the average melt rate flux; for the three-day period it averaged 50·4% of the average melt rate flux. Such large ground heat fluxes owing to heat conduction from the surface during snowmelt infiltration into frozen mineral soils are inconsistent with the small values found by coupled heat and mass transfer theory and measurement (Zhao and Gray, 1997; Zhao *et al.*, 1997).

CONCLUSIONS

The following conclusions are made with respect to snow processes in land surface models and the identification of the next phase of improvements in these models. Field data supporting the conclusions were largely collected from cold, relatively dry environments. Whilst the conclusions are normally applicable to other environments, application to global snow covers should consider any relevant differences in processes and energetics.

1. Snow interception by forests is either neglected or grossly underestimated by land surface models but can result in substantial canopy storage of snow (up to 60% of cumulative snowfall) and latent heat flux from snow-covered canopies. A process-based snow interception model for evergreen forests based on that developed by Hedstrom and Pomeroy (1998) is able to match measured interception and should be adopted.

2. Land surface models do not characterize blowing snow redistribution and sublimation. These processes can cause substantial differences (-40% to $+100\%$ difference) between accumulated snowfall and snow accumulation in prairie and arctic regions. Blowing snow sublimation losses are necessary to predict mean snow water equivalent at the grid scale, whilst blowing snow transport should be calculated to gain an appreciation of the subgrid variability of snow water equivalent.

3. With respect to snow density and snow densification it is recommended that:

   (i) the density of fresh snow be calculated as a function of temperature.

   (ii) the densification of well-exposed snow in areas subject to snow storms and blowing snow be treated as episodic. For non-melting snow and wind speeds greater than 7 m/s, increase snow density at a rate of 9 kg/m^3 h up to a maximum that is controlled by snow depth.

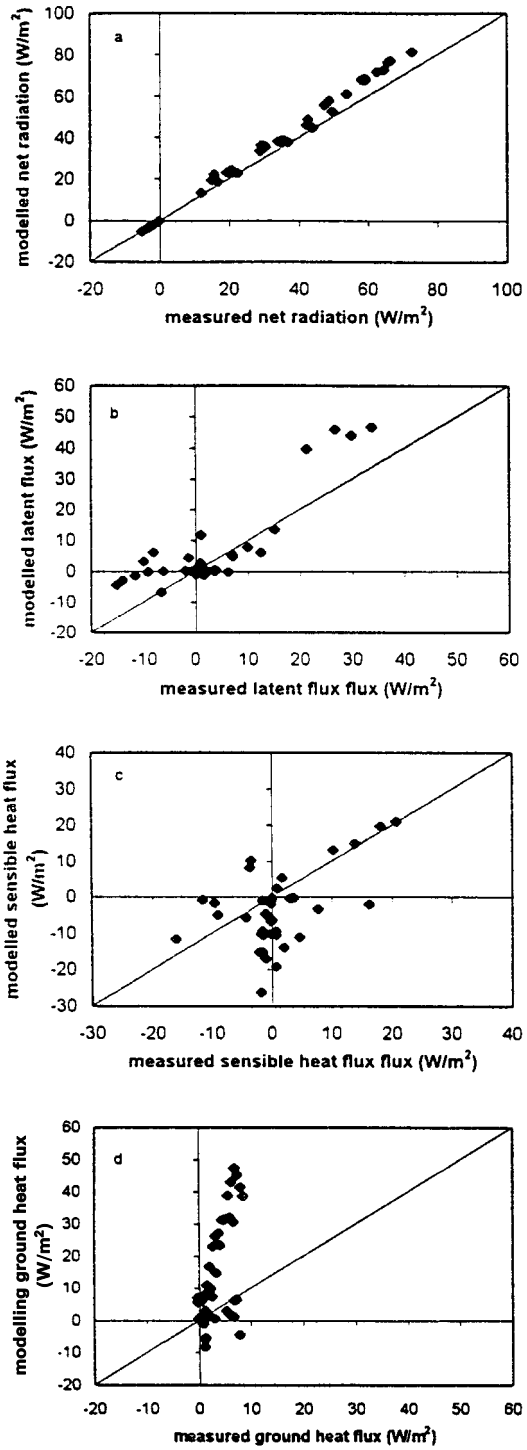

Figure 15. Comparison of 30-minute fluxes for periods of melt during 11–13 March 1996, Kernen Farm, near Saskatoon measured and modelled by CLASS: (a) net radiation, (b) latent energy, (c) sensible energy and (d) ground heat

(iii) for shallow, aged, wind-blown snow (mean depth, $d \leqslant 60$ cm) the mean density can be taken equal to 250 kg/m^3 (Shook and Gray, 1994). For deeper snow ($d > 60$ cm) the average density be calculated as a function of depth.

(iv) the maximum dry snow density for forested (boreal, mountain forest, maritime) environments can be set equal to 250 kg/m^3.

4. The two-parameter log–normal probability density function is recommended for describing the spatial distribution of snow water. This distribution requires knowledge of the mean and coefficient of variation of the water equivalent, CV. Initial estimates of CV can be derived from information on land cover and terrain features and the values provided in this paper.

5. Areal albedo and snow-covered area have a linear relationship during snowmelt. The snow albedo at the start of snow cover ablation should therefore not be altered during melt of the remaining snow cover. The decrease in snow-covered area can be calculated using the log–normal probability density function and an algorithm that applies calculated melt to reduce snow water equivalent and hence the area covered by snow.

6. Melt of isothermal, continuous open environment snow covers is largely driven by radiative fluxes. Turbulent transfer schemes in land surface models will attempt to calculate a turbulent contribution to melt that is larger than necessary.

7. Rapid and dramatic alterations to the soil temperature gradient during snowmelt are caused by the downward conduction of latent heat released by the refreezing of percolating meltwater in frozen soils. Therefore, the processes of heat and mass transfer into frozen soils during infiltration can only be described properly by a multi-layered soil model having a reasonably small grid spacing. For those land surface models with only a few soil layers, the ground heat flux during infiltration into frozen soils should not be calculated by estimating the temperature gradient. Instead, it is likely that the assumption of a very small value for ground heat or the use of parametric or empirical correlations for estimates of both the ground heat and infiltration will give better results.

8. One land surface model, CLASS, seriously underestimated the timing and rate of snowmelt in open environments despite having relatively sophisticated snowmelt and soil routines. The exact causes of the discrepancies are unknown but it appears that overestimation of the ground heat loss during infiltration to frozen soils is a primary factor. Errors in the other energy terms for melt are compensatory and partly a result of snowpack energetics, so correction of turbulent transfer and net radiation calculations in CLASS would further degrade the performance. It is recommended that further study of snow energetics and soil heat conduction during infiltration of meltwater into frozen soils be undertaken and the results incorporated into future land surface models. It is important in this procedure to establish carefully the reliability of the models in invoking closure of the energy equation.

ACKNOWLEDGEMENTS

The assistance of Dr Diana Verseghy in obtaining funding for this project, providing CLASS code and discussing the results is acknowledged. The authors wish to acknowledge the financial contributions of various agencies and organizations for funding that has been received in support of several studies whose results are summarized in this paper. They include: the Canadian Institute for Climate Studies, University of Victoria and Environment Canada — Land Surface Processes and GEWEX; the Natural Science and Engineering Research Council of Canada Operating Grants, Strategic Grants and Research Partnership Program; the Canadian GEWEX program; the Prince Albert Model Forest Association Inc. and the National Hydrology Research Institute. Dr Litong Zhao, Division of Hydrology, provided many helpful discussions regarding ground heat flux and infiltration into frozen soils. The authors also wish to recognize the substantial contribution to this study of field data collected by various individuals at the Division of

Hydrology and National Hydrology Research Institute over several decades, with particular reference to Mr Dell Bayne who collected and collated the data over the complete period of study.

REFERENCES

Benson, C. S. 1982. 'Reassessment of winter precipitation on Alaska's Arctic slope and measurements on the flux of wind-blown snow'. *Geophysical Institute Report UAG R-288*. Geophysical Institute, University of Alaska, Fairbanks, 26 pp.

Betts, A. K., Ball, J. H., Beljaars, A. C. M., Miller, M. J., and Viterbo, M. J. 1996. 'The land surface–atmosphere interaction: a review based on observational and global modelling perspectives', *J. Geophys. Res.*, **101**, 7209–7225.

Brown, T. and Pomeroy, J. W. 1989. 'A blowing snow particle detector', *Cold Regions Sci. Technol.*, **16**, 167–174.

Cess, R. D. et al. 1991. 'Interpretation of snow-climate feedbacks as produced by 17 general circulation models', *Science*, **253**, 888–892.

Chow, V. T. 1954. 'The log-probability law and its engineering applications', *Proc. Am. Soc. Civil Eng.*, **80**, 1–25.

de La Casinière, A. C. 1974. 'Heat exchange over a melting snow surface', *J. Glaciol.*, **13**, 55–72.

Donald, J. R. 1992. 'Snowcover depletion curves and satellite snowcover estimates for snowmelt runoff modelling'. *PhD Thesis*, University of Waterloo, Waterloo, Ontario, 232 pp.

Donald, J. R., Soulis, E. D., Kouwen, N., and Pietroniro, A. 1995. 'A land cover-based snow cover representation for distributed hydrological models', *Wat. Resour. Res.*, **31**, 995–1009.

Douville, H., Royer, J. F., and Mahfouf, J.-F. 1995. 'A new snow parameterization for the Meteo-France climate model, I, validation in stand-alone experiments', *Climate Dynam.*, **12**, 21–35.

Dyunin, A. K. 1959. 'Fundamentals of the theory of snow drifting', *Izvest. Sibirsk, Otdel, Akad. Nauk. USSR*, **12**, 11–24. [English translation by Belkov, G. 1961. *Technical Translation 952*. National Research Council of Canada, Ottawa],

Essery, R. L. H. 1997. 'Seasonal snow cover and climate change in the Hadley Centre GCM', *Ann. Glaciol.*, **25**, 362–366.

Goodison, B. E., Ferguson, H. L., and McKay, G. A. 1981. 'Measurement and data analysis', in Gray, D. M. and Male, D. H. (eds), *Handbook of Snow: Principles, Processes, Management and Use*. Pergamon Press, New York, pp. 191–274.

Goodison, B. E., Metcalfe, J. R., and Louie, P. Y. T. 1998. 'Summary of country analyses and results, Annex 5.B Canada', *The WMO Solid Precipitation Measurement Intercomparison Final Report, WMO/TD No. 872*. WMO, Geneva, pp. 105–112.

Granger, R. J. 1977. 'Energy exchange during melt of a prairie snowcover'. *MSc Thesis*, University of Saskatchewan, Saskatoon, 122 pp.

Granger, R. J. and Male, D. H. 1978. 'Melting of a prairie snowpack', *J. Appl. Meteorol.*, **17**, 1833–1842.

Gray, D. M. 1970. 'Snow hydrology of the prairie environment', in *Snow Hydrology, Proceedings of the Workshop Seminar*. Queen's Printer for Canada, Ottawa, pp. 21–34.

Gray, D. M. and Granger, R. J. 1988. 'Bad Lake Watershed: 1967–1986', in *Proceedings of the Canadian Hydrology Symposium No. 17: Canadian Research Basins, Successes, Failures and Future*. NRCC No. 30416., National Research Council of Canada, Associate Committee on Hydrology, Ottawa, pp. 143–154.

Gray, D. M. and Prowse, T. 1993. 'Snow and floating ice'. in Maidment D. R. (ed.), *Handbook of Hydrology*, McGraw-Hill Inc., New York, pp. 7.1–7.58.

Gray, D. M., Norum, D. I., and Dyck, G. E. 1970. 'Densities of prairie snowpacks'. Proc. 38th Annual Meeting Western Snow Conference, pp. 24–30.

Gray, D. M. et al. 1979. 'Snow accumulation and distribution', in Colbeck, S. C. and Ray, M. (eds), *Proceedings of Modelling Snow Cover Runoff*. US Army Cold Regions Research Laboratory, Hanover, pp. 3–33.

Gray, D. M., Landine, P. G., and Granger, R. J. 1985. 'Simulating infiltration into frozen Prairie soils in streamflow models', *Can. J. Earth Sci.*, **22**, 464–472.

Halberstram, I. and Schieldge, J. P. 1981. 'Anomalous behaviour of the atmospheric surface over a melting snowpack', *J. Appl. Meteorol.*, **20**, 255–265.

Harding, R. J. and Pomeroy, J. W. 1996. 'The energy balance of the winter boreal landscape', *J. Climate*, **9**, 2778–2787.

Hedstrom, N. and Pomeroy, J. W. 1998. 'Intercepted snow in the boreal forest: measurement and modelling', *Hydrol. Process.*, **12**, 1611–1625.

Hetherington, E. D. 1987. 'The importance of forests in the hydrological regime', in Healy, M. C. and Wallace, R. R. (eds), *Canadian Aquatic Resources*. Department of Fisheries and Oceans, Ottawa, pp. 179–211.

Jones, H. G. 1987. 'Chemical dynamics of snowcover and snowmelt in a boreal forest', in Jones, H. G. and Orville-Thomas, W. J. (eds), *Seasonal Snowcovers: Physics, Chemistry, Hydrology*. NATO ASI Series C(211), Reidel Publishing, Dordrecht, 531–574.

Kane, D. L. and Stein, J. 1983. 'Water movement into seasonally frozen soils', *Wat. Resour. Res.*, **19**, 1547–1557.

Karl, T. R., Groisman, P. Ya., Knight, R. W., and Heim, R. R. 1993. 'Recent variations of snow cover and snowfall in North America and their relation to precipitation and temperature variations', *J. Climate*, **6**, 1327–1344.

Li, L. and Pomeroy, J. W. 1997a. 'Estimates of threshold wind speeds for snow transport using meteorological data', *J. Appl. Meteorol.*, **36**, 205–213.

Li, L. and Pomeroy, J. W. 1997b. 'Probability of occurrence of blowing snow', *J. Geophys. Res.*, **102**, 21955–21964.

Liston, G. E. 1995. 'Local advection of momentum, heat and moisture during the melt of patchy snowcovers', *J. Appl. Meteorol.*, **34**, 1705–1715.

Loth, B., Graf, H.-F., and Oberhuber, J. M. 1993. 'Snow cover model for global climate simulations', *J. Geophys. Res.*, **98**, 10451–10464.

Lundberg, A. and Halldin, S. 1994. 'Evaporation of intercepted snow: analysis of governing factors', *Wat. Resour. Res.*, **30**, 2587–2598.

Male, D. H. 1980. 'The seasonal snowcover', in Colbeck S. C. (ed.), *Dynamics of Snow and Ice Masses*. Academic Press, New York, pp. 305–395.
Male, D. H. and Granger, R. J. 1979. 'Energy mass fluxes at the snow surface in a Prairie environment', in Colbeck, S. C. and Ray, M. (eds), *Proc. Modelling Snowcover Runoff*. US Army Cold Regions Research and Engineering Laboratory, Hanover. pp. 101–124.
Marsh, P. and Pomeroy, J. W. 1996. 'Meltwater fluxes at an arctic forest tundra site', *Hydrol. Process.*, **10**, 1383–1400.
Marsh, P. and Woo, M.-K. 1984. 'Wetting front advance and freezing of meltwater within a snow cover, 1, observations in the Canadian Arctic', *Wat. Resour. Res.*, **20**, 1853–1864.
Marsh, P., Pomeroy, J. W., and Neumann, N. 1997. 'Sensible heat flux and local advection over a heterogeneous landscape at an Arctic tundra site during snowmelt', *Ann. Glaciol.*, **25**, 132–136.
Marshall, S. and Oglesby, R. J. 1994. 'An improved snow hydrology for GCMs', *Climate Dynam.*, **10**, 21–37.
McFarlane, N. A., Boer, G. J., Blanchet, J.-P., and Lazare, M. 1992. 'The Canadian Climate Centre second generation circulation model and its equilibrium climate', *J. Climate*, **5**, 1013–1044.
O'Neill, A. D. J. 1972. 'The energetics of shallow prairie snowcovers'. *PhD Thesis*, University of Saskatchewan, Saskatoon, SK, 197 pp.
O'Neill, A. D. J. and Gray, D. M. 1973. 'Solar radiation penetration through snow', in *Proc. of UNESCO–WMO–IAHS Symposia on the Role of Snow and Ice in Hydrology*. Volume 1, IAHS Press, Wallingford, UK. pp. 227–249.
Pomeroy, J. W. 1989. 'A process-based model of snow drifting', *Ann. Glaciol.*, **13**, 237–240.
Pomeroy, J. W. and Dion, K. 1996. 'Winter radiation extinction and reflection in a boreal pine canopy: measurements and modelling', *Hydrol. Process.*, **10**, 1591–1608.
Pomeroy, J. W. and Goodison, B. E. 1997. 'Winter and snow', in Bailey, W. G., Oke, T. R., and Rouse, W. R. (eds), *The Surface Climates of Canada*. McGill–Queen's University Press, Montreal & Kingston, pp. 68–100.
Pomeroy, J. W. and Granger, R. J. 1997. 'Sustainability of the western Canadian boreal forest under changing hydrological conditions, I, snow accumulation and ablation', *Sustainability of Water Resources under Increasing Uncertainty*, *IAHS Publ.* **240**, IAHS Press, Wallingford. 237–242.
Pomeroy, J. W. and Gray, D. M. 1995. 'Snowcover accumulation, relocation and management'. *National Hydrology Research Institute Science Report No. 7*. NHRI, Environment Canada, Saskatoon, 144 pp.
Pomeroy, J. W. and Li, L. 1997. 'Development of the Prairie Blowing Snow Model for application in climatological and hydrological models'. In *Proceedings of the Eastern Snow Conference*. Vol. 54, pp. 186–197.
Pomeroy, J. W. and Schmidt, R. J. 1993. 'The use of fractal geometry in modelling intercepted snow accumulation and sublimation', in *Proc. Eastern Snow Conference*, Vol. 50, pp. 1–10.
Pomeroy, J. W., Gray, D. M., and Landine, P. G. 1993. 'The Prairie Blowing Snow Model: characteristics, validation, operation', *J. Hydrol.*, **144**, 165–192.
Pomeroy, J. W., Granger, R. J., Pietroniro, A., Elliott, J., Toth, B., and Hedstrom, N. 1997a. 'Hydrological pathways in the Prince Albert model forest'. *NHRI Contribution Series CS-97004*. NHRI, Saskatoon, 154 pp. + app.
Pomeroy, J. W., Marsh, P., and Gray, D. M. 1997b. 'Application of a distributed blowing snow model to the Arctic', *Hydrol. Process.*, **11**, 1451–1464.
Randall, D. A. et al. 1994. 'Analysis of snow feedbacks in 14 general circulation models', *J. Geophys. Res.*, **99**, 20757–20771.
Schmidt, R. A. 1972. 'Sublimation of wind-transported snow — a model', *Res. Pap. RM-90*. USDA Forest Service, Rocky Mountain Forest and Range Experimental Station, Fort Collins, 24 p.
Schmidt, R. A. and Gluns, D. R. 1991. 'Snowfall interception on branches of three conifer species', *Can. J. For. Res.*, **21**, 1262–1269.
Sellers, P. J., Randall, D. A., Collatz, G. J., Berry, J. A., Field, C. B., Dazlich, D. A., Zhang, C., Collelo, G. D., and Bounoua, L. 1996. 'A revised land surface parameterisation (SiB2) for atmospheric GCMs, part 1: model formation', *J. Climate*, **9**, 676–705.
Shook, K. 1993. 'Fractal geometry of snowpacks during ablation'. *MSc Thesis*, University of Saskatchewan, Saskatoon, 178 pp.
Shook, K. 1995. 'Simulation of the ablation of prairie snowcovers'. *PhD Thesis*, University of Saskatchewan, Saskatoon, 189 pp.
Shook, K. and Gray, D. M. 1994. 'Determining the snow water equivalent of shallow prairie snowcovers', in *Proc. 51st Annual Meeting Eastern Snow Conference*, Dearborn, MI, pp. 89–95.
Shook, K. and Gray, D. M. 1997. 'Snowmelt resulting from advection', *J. Hydrol. Process.*, **11**, 1725–1736.
Shook, K., Gray, D. M., and Pomeroy, J. W. 1993. 'Temporal variation in snowcover area during melt in Prairie and Alpine environments', *Nord. Hydrol.*, **24**, 183–198.
Shook, K., Gray, D. M., and Pomeroy, J. W. 1994. 'Geometry of patchy snowcovers', *Proc. 1993 Annual Meeting Eastern Snow Conference June 8–10, 1993, Quebec City*, pp. 89–96.
Steppuhn, H. and Dyck, G. E. 1974. 'Estimating true basin snowcover', in *Advanced Concepts and Techniques in the Study of Snow and Ice Resources*. National Academy of Science, Washington, DC, pp. 314–328.
Sturm, M. 1992. 'Snow distribution and heat flow in the taiga', *Arc. Alp. Res.*, **24**, 145–152.
Tabler, R. D., Pomeroy, J. W., and Santana, B. W. 1990. 'Drifting snow', in Ryan, W. L. and Crissman, R. D. (eds), *Cold Regions Hydrology and Hydraulics*. Am. Soc. Civil Eng., New York, pp. 95–146.
Thomas, G. and Rowntree, P. R. 1992. 'The boreal forest and climate', *Q. J. R. Meteorol. Soc.*, **118**, 469–498.
US Army Corps of Engineers 1956. *Snow Hydrology: Summary Report of the Snow Investigations*, North Pacific Division, Portland, 437 pp.
Verseghy, D. L. 1991. 'CLASS — a Canadian land surface scheme for GCMs I. Soil model', *Int. J. Climatol.*, **11**, 111–133.
Verseghy, D. L., McFarlane, N. A., and Lazare, M. 1993. 'CLASS — a Canadian land surface scheme for GCMs II. Vegetation model and coupled runs', *Int. J. Climatol.*, **13**, 347–370.
Viterbo, P. and Beljaars, A. C. M. 1995. 'An improved land surface parameterisation scheme in the ECMWF model and its validation', *J. Climate*, **8**, 2716–2748.
Webb, E. K. 1970. 'Profile relationships: the log–linear range and extension to strong stability', *Q. J. R. Meteorol. Soc.*, **96**, 67–90.
Wiscombe, W. J. and Warren, S. G. 1980. 'A model for the spectral albedo of snow, I, pure snow', *J. Atmos. Sci.*, **37**, 2712–2733.

Woo, M.-K. 1990. 'Permaforst hydrology', in Prowse, T. D. and Ommaney, C. S. L. (eds), *Northern Hydrology: Candian Perspectives*. NHRI Science Report No. 1. Minister of Supply and Services, Canada, Saskatoon, pp. 63–76.
Woo, M.-K, and Marsh, P. 1977. 'Determination of snow storage for small eastern high Arctic basins', in *Proc. 1977 Annual Meeting Eastern Snow Conference, Feb. 3–4, Belleville*, pp. 147–162.
Woo, M.-K. and Steer, P. 1986. 'Monte Carlo simulation of snow depth in a forest', *Wat. Resour. Res.*, **22**, 864–868.
Woo, M.-K., Heron, R., and Marsh, P. 1982. 'Basal ice in high arctic snowpacks', *Arc. Alp. Res.*, **14**, 251–260.
Yen, Y.-C. 1995. 'Sensible heat flux measurements near a cold surface', in *Report 95-22*. US Army Cold Regions Research and Engineering Laboratory, Hanover, 42 pp.
Zhao, L. and Gray, D. M. 1997. 'A parametric expression for estimating infiltration into frozen soils', *Hydrol. Process.*, **11**, 1761–1775.
Zhao, L., Gray, D. M., and Male, D. H. 1997. 'Numerical analysis of simultaneous heat and mass transfer during infiltration into frozen ground', *J. Hydrol.*, **200**, 345–363.

